ANALYSIS OF A PARABOLIC WAVEGUIDE WITH ROTATIONALLY SYMMETRIC EXCITATION

by

Joseph LoVetri

A Thesis
Presented to the Faculty of Graduate Studies
University of Manitoba

In Partial Fulfillment
of the Requirements for the Degree
Master of Science
in
Electrical Engineering

ISBN 0-315-33820-2

ANALYSIS OF A PARABOLIC WAVEGUIDE WITH ROTATIONALLY SYMMETRIC EXCITATION

BY

JOSEPH LOVETRI

A thesis submitted to the Faculty of Graduate Studies of the University of Manitoba in partial fulfillment of the requirements of the degree of

MASTER OF SCIENCE

ABSTRACT

In this thesis the problem of the circular paraboloidal waveguide is analyzed. It is shown how the Coulomb wave functions, commonly used in the description of a Coulomb field surrounding a nucleus, can be used in the description of electromagnetic fields which are symmetric with respect to the azimuthal coordinate inside the waveguide. The Abraham potentials Q and U,which are useful in describing fields with rotational symmetry, are used to simplify the problem. It is shown that these potentials must satisfy a partial differential equation which when separated yields the Coulomb wave equation of order L=0. Electromagnetic fields due to simple source distributions inside the paraboloid are expanded in terms of these functions . Specifically, solutions for current loop sources located in the focal plane of the paraboloid are obtained. The case where the wall of the paraboloidal waveguide is assumed to be perfectly conducting is treated as well as the case where the wall has finite impedance. The finite paraboloid is also considered and the far field is formulated using Huygen's principle. It is found that for the finite surface impedance case the far field pattern due to a current loop operating at 100 MHz in the focal plane is different than for the perfectly conducting case. Numerical results are presented for relevant aspects of the problem.

ACKNOWLEDGEMENTS

The author would like to express his deep appreciation to Dr. M. Hamid for suggesting the problem and for the guidance throughout the project. It is also with sincere gratitude that the author would like to acknowledge Dr. D.W. Trim for his helpful discussions during the completion of this work. Appreciation is also extended to Dr. F.M. Arscott for the invaluable and profitable time he spent with the author and for his kind help in the writing of Appendix A.

The author is also gratefull to the Natural Sciences and Engineering Research Council of Canada for their financial assistance in this project.

The greatest debt is owed to my wife Karen and to my children for their endless patience and understanding. No words could possibly begin to express my gratitude towards them.

TABLE OF CONTENTS

LIST OF TABLES

LIST OF FIGURES

LIST OF PRINCIPAL SYMBOLS

i	$\sqrt{-1}$
ω	harmonic frequency
ϵ	permitivity
μ	permeability
ρ_c	charge density of the region
σ	conductivity of the region
e	base of the natural logarithm (2.718281828...)
$e^{-i\omega t}$	time dependence
(x, y, z)	Cartesian coordinates
(ρ, ϕ, z)	circular cylindrical coordinates
(r, θ, ϕ)	spherical coordinates
(ξ, η, ϕ)	rotation-paraboloidal coordinates
(ξ_1, ξ_2, ξ_3)	general curvilinear coordinates
(h_1, h_2, h_3)	scale factors or metric coefficients
N^2	normalization constant for eigenfunctions
$\ddot{N}$	dyadic relative surface impedance
N_u	normalization constant for relative radiation intensity
K	wave number
π	3.141592653...
γ	*Euler's* number

λ	wavelength or eigenvalue
$F_0(\beta, z)$	regular Coulomb wave function with parameter β, argument z
$G_0(\beta, z)$	irregular Coulomb wave function with parameter β, argument z
$H_0^1(\beta, z)$	wave function of the third kind with parameter β, and argument z for outward travelling waves
$H_0^2(\beta, z)$	wave function of the third kind with parameter β, and argument z for inward travelling waves
$\hat{n}$	outward unit vector normal to a conducting surface
$\bar{H}$	total magnetic field vector
$\bar{H}_1$	total magnetic field outside surface S
H_ξ	ξ component of the magnetic field vector
H_η	η component of the magnetic field vector
J_ϕ	ϕ directed linear current density
$\bar{E}$	total electric field vector
$\bar{E}_1$	total electric field outside surface S
E_ξ	ξ component of electric field vector
E_ϕ	ϕ component of electric field vector
$\bar{J}(\xi, \eta)$	general current density inside paraboloid
(ξ^*, η^*)	location of current loop inside paraboloid
η_0	constant surface of paraboloid
ξ_0	aperture surface of finite paraboloid
f	focal length of paraboloid

A_n	coefficient in generalized Fourier series expansion
B_n	coefficient in generalized Fourier series expansion
$U(\xi, \eta)$	Abraham potential for T.E. field
$Q(\xi, \eta)$	Abraham potential for T.M. field
$\bar{L}$	longitudinal Hansen wave vector
$\bar{M}$	transverse Hansen wave vector
$\bar{N}$	transverse Hansen wave vector
$\bar{A}$	magnetic vector potential
$\bar{F}$	electric vector potential
$\bar{N}_A$	radiation vector
$\bar{L}_F$	radiation vector

CHAPTER I

INTRODUCTION

Paraboloidal reflector antennas are perhaps the most useful and widely used antennas for communication purposes. The majority of satellite communication links use paraboloidal reflector antennas. The most common type of reflector is the circular parabolic type which has a surface generated by revolving a finite parabolic curve about its axis. The reflector is then usually illuminated by an electromagnetic source positioned at or near the focal point. The reason for using the circular paraboloidal reflector is that from the theory of geometrical optics or ray optics the circular paraboloidal shape has the property that all rays originating from the focus are reflected from the surface parallel to the axis. Most electromagnetic solutions of the paraboloidal reflector use the geometrical optics approximation. This is in general a high frequency method and thus it is not an exact solution.

The two main techniques which are widely used in the analysis of the paraboloidal reflector consist of

1. using ray optics to find the field on the aperture plane, which is the circular aperture just in front of the paraboloid, and then Huygen's principle is used to determine the far field of the antenna,

or

2. determining the surface currents on the paraboloidal surface due to the original source and then finding the radiated field from these using for example the auxiliary magnetic and electric vector potentials.

These two techniques may be found in many current textbooks of antenna theory or electromagnetics and will not be discussed in this thesis (see for example Balanis [1982], or Stutzman and Thiele [1981]).

One of the classic methods of determining exact solutions in electromagnetic problems is to solve Maxwell's equations directly for the geometry, material and sources under consideration. Solving Maxwell's equations can usually be reduced to finding the solutions of the vector wave equation or, for time harmonic problems, the vector Helmholtz equation. It would probably be safe to say that most electromagnetic solutions are directly or indirectly related to the solution of the vector wave equation.

One very powerful method for solving scalar partial differential equations is the method of separation of variables. Thus if the vector wave equation can be broken up into scalar equations then the method of separation of variables could be used to solve each of these scalar equations.

In terms of the orthogonal coordinate systems in which solutions can be obtained, the scalar Helmholtz equation can be solved using the method of separation of variables in eleven orthogonal coordinate systems. The rotation-paraboloidal coordinate system is one of the eleven orthogonal coordinate systems in which the scalar Helmholtz equation separates (see Eisenhart [1934], Stratton [1941], Morse and Feshbach [1953]). The situation is quite different with the vector wave equation or the vector Helmholtz equation (see Moon and Spencer [1971]). The complications arise because the field is a vector field and the vector equation can not be separated into individual ordinary differential equations in which each scalar component exists decoupled from the remaining components. Also, even if this were possible, the fitting of the boundary conditions becomes almost impossible.

In this introduction we will review the general curvilinear coordinate systems in preparation for our work with the rotation-paraboloidal coordinate system. We will also try to summarize the electromagnetic and acoustic scattering studies which have been done in the past in the rotation-paraboloidal system (for an excellent summary see Bowman et.al. [1969]). The methods used previously are not given in any detail here since the form of the analysis presented in this thesis is independent of those

methods. Only a general survey of those methods is presented in order that an overall picture of what has been done can be obtained.

1.1 General Curvilinear Coordinates

In general curvilinear coordinates (ξ_1, ξ_2, ξ_3) the vector operations such as curl and divergence are expressed in terms of metric coefficients or scale factors (h_1, h_2, h_3) which are determined by the expressions governing the transformation from the coordinates of interest to the rectangular coordinates (x, y, z). The scale factors can be determined by applying

$$(h_i)^2 = \left(\frac{\partial x}{\partial \xi_i}\right)^2 + \left(\frac{\partial y}{\partial \xi_i}\right)^2 + \left(\frac{\partial z}{\partial \xi_i}\right)^2 \qquad i = 1,2,3. \tag{1.1}$$

The rotation-paraboloidal coordinate system (ξ, η, ϕ), see Fig. 1.1, is related to the rectangular coordinate system (x, y, z), the circular cylindrical coordinate system (ρ, ϕ, z), and the spherical coordinate system (r, θ, ϕ) by the transformations

$$x = \xi\eta\cos\phi = \rho\cos\phi = r\sin\theta\cos\phi \ , \tag{1.2}$$

$$y = \xi\eta\sin\phi = \rho\sin\phi = r\sin\theta\sin\phi \ , \tag{1.3}$$

$$z = \frac{1}{2}(\xi^2 - \eta^2) = z = r\cos\theta \ . \tag{1.4}$$

Thus the scale factors are obtained by applying Eq. (1.1) to the above equations with the result that

$$h_1 = h_2 = \sqrt{\xi^2 + \eta^2} = 2r \ , \tag{1.5}$$

and

$$h_3 = \xi\eta = \rho \ , \tag{1.6}$$

where, of course, $\rho^2 = x^2 + y^2$ and $r^2 = x^2 + y^2 + z^2$.

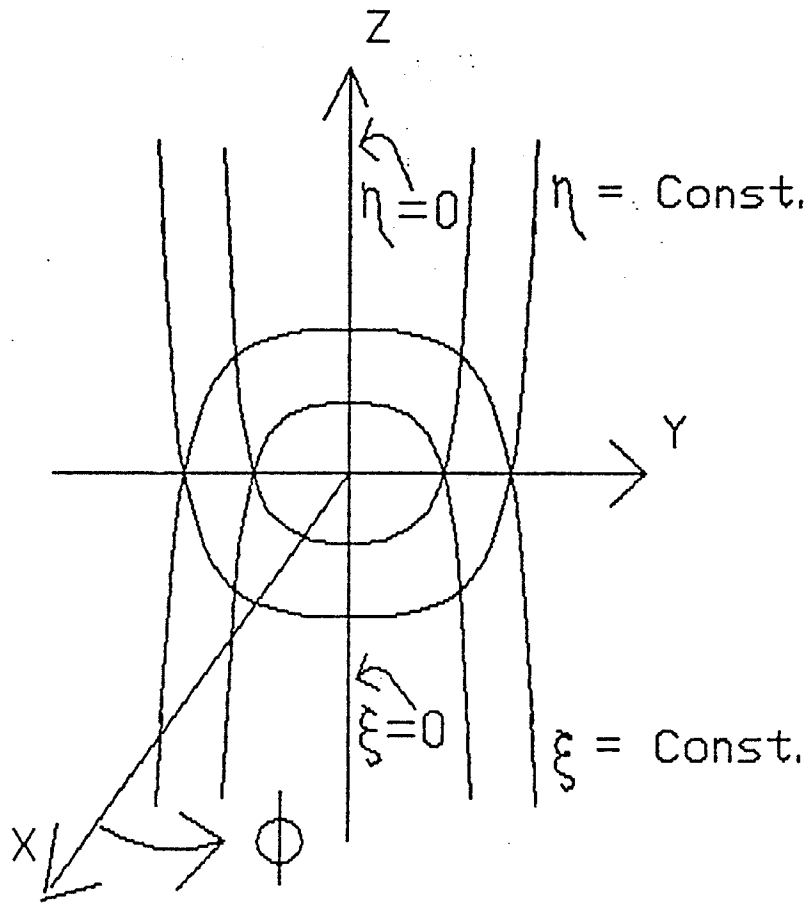

FIG. 1.1: ROTATION-PARABOLOIDAL COORDINATES

The scalar Helmholtz equation is given by :

$$\nabla^2\psi + K^2\psi = 0 \ , \tag{1.7}$$

where ψ is the actual scalar field or potential. This equation can be written for a general curvilinear coordinate system for the field $\psi(\xi_1, \xi_2, \xi_3)$ as

$$g^{-1/2} \sum_{i=1}^{3} \frac{\partial}{\partial \xi_i} \left[\frac{g^{1/2}}{h_i^2} \frac{\partial \psi}{\partial \xi_i} \right] + K^2\psi = 0 \tag{1.8}$$

where

$$\sqrt{g} = h_1 h_2 h_3 \ . \tag{1.9}$$

Now in the analysis of electromagnetic fields we encounter frequently the vector Helmholtz equation which is of the form

$$\overline{\nabla} \times \overline{\nabla} \times \overline{F} - K^2 \overline{F} = 0 \tag{1.10}$$

and is derived from the vector wave equation by assuming a harmonic time dependence given by $e^{-i\omega t}$ where ω is the harmonic frequency. Now for a rectangular, Cartesian system of coordinates (x, y, z) it is clear that Eq. (1.10) reduces to the scalar Helmholtz equation for each component in that system, but for other orthogonal coordinate systems this is not the case. In fact, there is generally great difficulty in separating the vector Helmholtz equation if one is not working in Cartesian coordinates.

It was shown by Hansen (see Hansen [1953]),that the vector wave equation can be separated by defining three new vector fields related to the actual vector fields of interest. These three vector fields $\overline{M}, \overline{N}, \overline{L}$ (known as the Hansen wave vectors), can be obtained by a single scalar field ψ, which satisfies the scalar wave equation in the coordinate system of interest. Separation of the vector wave equation has sometimes been defined as the successful deduction of the Hansen wave vectors (Morse

and Feshbach [1953], pp. 1767). It has been shown that the Hansen wave vectors can be obtained for only six of the eleven orthogonal coordinate systems. These six coordinate systems are shown below in Table 1. Unfortunately the rotation paraboloidal coordinate system is not one of six given in Table 1, and thus complications arise in the solution of electromagnetic fields in this coordinate system.

Table 1.1
Coordinate Systems in which Vector Wave Equation Separates
1. rectangular coordinates
2. circular cylindrical coordinates
3. elliptic cylindrical coordinates
4. parabolic cylindrical coordinates
5. spherical coordinates
6. conical coordinates

1.2 The Rotation-Paraboloidal Coordinate System

The first theoretical investigation of electromagnetic fields in rotation-paraboloidal coordinates was undertaken by Abraham [1900]. The paraboloidal coordinates were used to model a semi-infinite wire. The theoretical results did not agree with the experimental results of the time and the problem was dropped. The electromagnetic reflection by a parabolic mirror was briefly mentioned by Lamb [1906] where integral expressions were obtained. The problem was not reconsidered until the parabolic reflector was used for radar applications in the 1940's.

For the acoustic case Buchholtz analyzed many aspects of the problem. He obtained results in integral and series form for the scattering of acoustic waves from an infinite paraboloid (Buchholtz [1947]). The external (convex side) diffraction

problem has been analyzed by Horton [1950, 1953]. Horton used the series representations developed by Pinney [1946] for the solution of the scalar Helmholtz equation in rotation-paraboloidal coordinates. Pinney developed his series representation in terms of Laguerre functions whereas Buchholtz used the confluent hypergeometric functions which are a more general form.

Analysis of the electromagnetic case was made based on the results from the acoustic case. The cases of an electric dipole at the focus of the paraboloid and oriented parallel to the axis of symmetry, perpendicular to the axis of symmetry, and perpendicular to the axis backed by a dummy reflector were solved by Pinney [1947]. The solutions to these three cases were based on the series solutions he obtained in his earlier paper for the scalar Helmholtz equation in rotation-paraboloidal coordinates. The exact electromagnetic field produced by an electric dipole located on the axis of symmetry of a perfectly conducting concave paraboloid has also been solved by Buchholtz [1948]. Fock [1965] has performed an in depth study of the problem, expressing the exact solution for an electric dipole at the focus and perpendicular to the axis of symmetry, both as an integral and as an infinite series, as well as deriving high frequency expansions.

In his investigations, Fock introduces a series of new potentials in order to solve the problem. He first expresses Maxwell's equations in terms of the covariant spherical field components and the Debye potentials (see Wilcox [1957]). From these he applies the transformation to obtain the rotation-paraboloidal field components. He then introduces two " parabolic potentials P and Q " which are connected with the separate Fourier components of the field with respect to the angle ϕ, and not the total field. To simplify the field expressions, four interrelated auxiliary functions connected with the parabolic potentials P and Q are introduced. Although the introduction of the parabolic potentials permits formulation of the boundary conditions without recourse to finite difference equations the expressions are very complicated even for simple source illuminations.

The problem under consideration in Horton and Karal's work was the electromagnetic scattering of a plane wave from a paraboloid made of any material in general (Horton and Karal [1951]). The Hansen wave vectors were obtained for the rotation-paraboloidal coordinate system based on the series solution obtained by Pinney [1946] for the scalar Helmholtz equation. This was done even though the transverse wave vectors $\overline{M}$ and $\overline{N}$ did not appear to have the necessary orthogonality properties to enable one to expand an arbitrary vector function in terms of them directly. Considerable manipulations were then performed in order to use the orthogonality properties of one of Pinney's paraboloidal functions S_{ν}^{μ} (S_{ν}^{μ} is related to the Laguerre functions). The final field expressions using this method are very complicated. Solutions for a plane wave incident upon a perfectly conducting paraboloid are formulated but no numerical results are presented because of a " lack of numerical values for the paraboloidal functions ".

Approximate methods have been used by Donaldson et.al. [1960] to solve for the aperture distribution due to axially oriented dipoles at the focal point. An approximate method is used to obtain the coupling between two aligned paraboloidal reflectors. These approximate methods are based on Fourier transforms of the aperture field.

The high frequency methods of geometrical optics and ray tracing will not be discussed since they represent a totally different approach to the problem.

In this thesis the paraboloid of revolution is treated as a waveguide and fields which are rotationally symmetric but arbitrary (ie. the field components are independent of ϕ) are found in terms of the Abraham potentials (see Stratton [1941] or Koshlyakov et.al. [1964]). Eigenfunctions are obtained for the paraboloid in terms of the Coulomb wave functions. This technique of treating the paraboloid as a waveguide allows one to to apply an impedance boundary condition on the walls of the paraboloid. This is a technique which can be used for simulating mathematically the finite conductivity of the walls or can even be used when deliberate thin coatings

of dielectric are applied to the walls. This problem is difficult to solve if geometrical optics is used but means only the determination of the new eigenvalues in the present technique. Thus for each new boundary condition we wish to solve (ie. different wall impedance) all that need be done is to calculate the new eigenvalues. This is one of the main advantages of this method.

CHAPTER 2

GENERAL FORMULATION WITH ABRAHAM POTENTIALS

Given the coordinate transformations of Eq. (1.2) - (1.6), Maxwell's equations are obtained for the rotation-paraboloidal coordinate system. The Abraham potentials Q and U are then used to simplify the solution of these equations when rotational symmetry of the fields is evident. The partial differential equations for these potentials are then separated, yielding one Sturm-Liouville system and one ordinary differential equation. It is shown that solutions to both of these can be represented most conveniently as Coulomb wave functions.

2.1 Maxwell's Equations in Rotation-Paraboloidal Coordinates

If a harmonic time dependence of $e^{-i\omega t}$ is assumed then Maxwell's equations can be written as

$$\nabla \times \bar{E} = i\,\omega\,\mu\,\bar{H}\ , \tag{2.1}$$

$$\nabla \times \bar{H} = (-i\,\omega\,\epsilon + \sigma)\bar{E}\ ,$$

$$\nabla \times \bar{H} = -i\,\omega\,\epsilon\,\bar{E}\ \ (\textit{lossless medium}), \tag{2.2}$$

$$\nabla \cdot \bar{H} = 0\ , \tag{2.3}$$

$$\nabla \cdot \bar{E} = \frac{\rho_c}{\epsilon}\ . \tag{2.4}$$

Where ρ_c is the charge density in the medium, ϵ is the permitivity of the medium, μ is the permeability of the medium and ω is the harmonic frequency of the excitation. These must now be expressed in terms of the rotation-paraboloidal coordinate system but first these expressions will be determined for any rotationally symmetric

coordinate system.

Any system of coordinates (ξ, η, ϕ) which are rotationally symmetric can be defined by

$$ds^2 = h_1 d\xi^2 + h_2 d\eta^2 + \rho^2 d\phi^2,$$

where ρ is the perpendicular distance from the axis of rotation (ie. the same as in cylindrical coordinate systems). Maxwell's equations, Eq. (2.1) and (2.2), for an isotropic lossless medium can be written in these coordinate systems as

$$\frac{1}{h_2 \rho}\left[\frac{\partial}{\partial \eta}\left(\rho \begin{matrix} H_\phi \\ E_\phi \end{matrix}\right) - \frac{\partial}{\partial \phi}\left(h_2 \begin{matrix} H_\eta \\ E_\eta \end{matrix}\right)\right] \pm i\omega \begin{pmatrix} \epsilon E_\xi \\ \mu H_\xi \end{pmatrix} = 0, \tag{2.5a}$$

$$\frac{1}{h_1 \rho}\left[\frac{\partial}{\partial \phi}\left(h_1 \begin{matrix} H_\xi \\ E_\xi \end{matrix}\right) - \frac{\partial}{\partial \xi}\left(\rho \begin{matrix} H_\phi \\ E_\phi \end{matrix}\right)\right] \pm i\omega \begin{pmatrix} \epsilon E_\eta \\ \mu H_\eta \end{pmatrix} = 0, \tag{2.5b}$$

$$\frac{1}{h_1 h_2}\left[\frac{\partial}{\partial \xi}\left(h_2 \begin{matrix} H_\eta \\ E_\eta \end{matrix}\right) - \frac{\partial}{\partial \eta}\left(h_1 \begin{matrix} H_\xi \\ E_\xi \end{matrix}\right)\right] \pm i\omega \begin{pmatrix} \epsilon E_\phi \\ \mu H_\phi \end{pmatrix} = 0, \tag{2.5c}$$

where for the case of rotational-paraboloidal coordinates h_1 and h_2 are equal and are defined by Eq. (1.5). For the case where the field ($\bar{E}$ and $\bar{H}$) itself has the same symmetry as the coordinate system, its components are independent of ϕ. Thus the six expressions of Eq. (2.5) break up into the two independent groups

$$\frac{1}{h_1 h_2}\left[\frac{\partial}{\partial \xi}\left(h_2 H_\eta\right) - \frac{\partial}{\partial \eta}\left(h_1 H_\xi\right)\right] + i\omega \epsilon E_\phi = 0, \tag{2.6a}$$

$$\frac{1}{\rho h_2}\frac{\partial}{\partial \eta}\left(\rho E_\phi\right) - i\omega \mu H_\xi = 0, \tag{2.6b}$$

$$\frac{1}{\rho h_1}\frac{\partial}{\partial \xi}\left(\rho E_\phi\right) + i\omega \mu H_\eta = 0, \tag{2.6c}$$

and

$$\frac{1}{h_1 h_2}\left[\frac{\partial}{\partial \xi}\left(h_2 E_\eta\right) - \frac{\partial}{\partial \eta}\left(h_1 E_\xi\right)\right] - i\,\omega\,\mu H_\phi = 0\,, \tag{2.7a}$$

$$\frac{1}{\rho h_2}\frac{\partial}{\partial \eta}\left(\rho H_\phi\right) + i\,\omega\,\epsilon E_\xi = 0\,, \tag{2.7b}$$

$$\frac{1}{\rho h_1}\frac{\partial}{\partial \xi}\left(\rho H_\phi\right) - i\,\omega\,\epsilon E_\eta = 0\,. \tag{2.7c}$$

For the specific case of the rotation-paraboloidal coordinates Eq. (2.6) and (2.7) become

$$\frac{1}{\xi^2+\eta^2}\left[\frac{\partial}{\partial \xi}\left(\sqrt{\xi^2+\eta^2}H_\eta\right) - \frac{\partial}{\partial \eta}\left(\sqrt{\xi^2+\eta^2}H_\xi\right)\right] + i\,\omega\,\epsilon E_\phi = 0, \tag{2.8a}$$

$$\frac{1}{\rho\sqrt{\xi^2+\eta^2}}\frac{\partial}{\partial \eta}\left(\rho E_\phi\right) - i\,\omega\,\mu H_\xi = 0, \tag{2.8b}$$

$$\frac{1}{\rho\sqrt{\xi^2+\eta^2}}\frac{\partial}{\partial \xi}\left(\rho E_\phi\right) + i\,\omega\,\mu H_\eta = 0. \tag{2.8c}$$

and,

$$\frac{1}{\xi^2+\eta^2}\left[\frac{\partial}{\partial \xi}\left(\sqrt{\xi^2+\eta^2}E_\eta\right) - \frac{\partial}{\partial \eta}\left(\sqrt{\xi^2+\eta^2}E_\xi\right)\right] - i\,\omega\,\mu H_\phi = 0, \tag{2.9a}$$

$$\frac{1}{\rho\sqrt{\xi^2+\eta^2}}\frac{\partial}{\partial \eta}\left(\rho H_\phi\right) + i\,\omega\,\epsilon E_\xi = 0, \tag{2.9b}$$

$$\frac{1}{\rho\sqrt{\xi^2+\eta^2}}\frac{\partial}{\partial \xi}\left(\rho H_\phi\right) - i\,\omega\,\epsilon E_\eta = 0, \tag{2.9c}$$

where $\rho = \xi\,\eta$. Substituting Eq. (2.8b) and (2.8c) into Eq. (2.8a), and defining the Abraham potential $U\,(\xi\,,\eta)$ as

$$E_\phi(\xi\,,\eta) = \frac{1}{\rho}U\,(\xi\,,\eta)\,, \tag{2.10}$$

it is found that

$$H_{\xi}(\xi,\eta) = \frac{-i\,\omega\epsilon}{\rho K^2\sqrt{\xi^2+\eta^2}}\,\frac{\partial U(\xi,\eta)}{\partial \eta}\,, \tag{2.11}$$

$$H_{\eta}(\xi,\eta) = \frac{i\,\omega\epsilon}{\rho K^2\sqrt{\xi^2+\eta^2}}\,\frac{\partial U(\xi,\eta)}{\partial \xi}\,, \tag{2.12}$$

where $U(\xi,\eta)$ satisfies

$$\frac{\partial}{\partial \xi}\left(\frac{1}{\rho}\,\frac{\partial U}{\partial \xi}\right) + \frac{\partial}{\partial \eta}\left(\frac{1}{\rho}\,\frac{\partial U}{\partial \eta}\right) + \frac{K^2}{\rho}\left(\xi^2+\eta^2\right)U = 0\,. \tag{2.13}$$

Similarly if the same procedure is applied to Eq.(2.9) the second Abraham potential $Q(\xi,\eta)$ can be defined as

$$H_{\phi}(\xi,\eta) = \frac{1}{\rho}Q(\xi,\eta)\,, \tag{2.14}$$

with

$$E_{\xi}(\xi,\eta) = \frac{i\,\omega\mu}{\rho K^2\sqrt{\xi^2+\eta^2}}\,\frac{\partial Q(\xi,\eta)}{\partial \eta}\,, \tag{2.15}$$

$$E_{\eta}(\xi,\eta) = \frac{-i\,\omega\mu}{\rho K^2\sqrt{\xi^2+\eta^2}}\,\frac{\partial Q(\xi,\eta)}{\partial \xi}\,, \tag{2.16}$$

where $Q(\xi,\eta)$ satisfies

$$\frac{\partial}{\partial \xi}\left(\frac{1}{\rho}\,\frac{\partial Q}{\partial \xi}\right) + \frac{\partial}{\partial \eta}\left(\frac{1}{\rho}\,\frac{\partial Q}{\partial \eta}\right) + \frac{K^2}{\rho}\left(\xi^2+\eta^2\right)Q = 0\,. \tag{2.17}$$

It can be easily seen from the above expressions that the potential $U(\xi,\eta)$ represents an electromagnetic wave which is transverse electric to the z direction (T.E. to z) and the second potential $Q(\xi,\eta)$ represents an electromagnetic wave which is transverse magnetic to the z direction (T.M. to z). It should also be

observed that both U and Q satisfy the same partial differential equation, Eq. (2.13) and Eq. (2.17). This suggests that the form of the solutions to the potentials U and Q should be similar but not exactly the same since the boundary conditions on the walls of the paraboloid will not necessarily be the same for both potentials. It can also be noted at this point that there is the possibility of a singularity in the field along the axis of the parabaloid due to the forms of the expressions of Eq. (2.10) and (2.14) since $\rho = 0$ along this axis. It will turn out that the solutions to the potentials will be chosen such that they are equal to zero at $\rho = 0$ and in the limit as ρ goes to zero the field expressions will not be singular but finite.

All of the above observations and comments will be detailed in following chapters.

2.2 Boundary Conditions for the Potentials

2.2.1 Perfectly Conducting Paraboloid

If the surface of the paraboloid ($\eta = \eta_o$) is perfectly conducting then the mathematical expression which conveys this is

$$\bar{E} - (\bar{E} \cdot \hat{n})\hat{n} = 0 , \tag{2.18}$$

where $\hat{n}$ is the unit normal to the surface directed from the body into the surrounding medium. Physically Eq. (2.18) states that the tangential component of the total electric field at any regular point of the conducting surface must be equal to zero. For the case of the paraboloid

$$\hat{n} = -\hat{a}_\eta . \tag{2.19}$$

Thus Eq. (2.18) becomes

$$\bar{E} - (\bar{E} \cdot \hat{a}_\eta)\hat{a}_\eta = 0 . \tag{2.20}$$

The field $\bar{E}(\xi, \eta)$ can be represented as

$$\bar{E}(\xi,\eta) = E_\xi \hat{a}_\xi + E_\eta \hat{a}_\eta + E_\phi \hat{a}_\phi \,. \tag{2.21}$$

Substituting Eq. (2.21) into Eq. (2.20) results in what was originally expected, i.e.

$$E_\xi(\xi,\eta) = 0\,, \tag{2.22}$$

and

$$E_\phi(\xi,\eta) = 0\,. \tag{2.23}$$

From Eq. (2.22) and (2.15) a Neumann condition for the potential $Q(\xi,\eta)$ arises;

$$\frac{\partial Q(\xi,\eta)}{\partial \eta} = 0 \qquad at\ \eta = \eta_o\,, \tag{2.24}$$

and from Eq. (2.23) and (2.10) a Dirichlet condition for the potential $U(\xi,\eta)$ arises;

$$U(\xi,\eta_o) = o\,. \tag{2.25}$$

Thus for the perfectly conducting paraboloidal waveguide, described by the coordinate surface $\eta = \eta_o$, the Abraham potentials $U(\xi,\eta)$ and $Q(\xi,\eta)$ must satisfy partial differential equations given by Eq. (2.13) and Eq. (2.17) respectively, with boundary conditions at $\eta = \eta_o$ described by Eq. (2.25) and Eq. (2.24) respectively.

2.2.2 Non-Perfectly Conducting Paraboloid

For the case of the walls of the paraboloidal waveguide being non-perfectly conducting, an Impedance or Leontovich boundary condition is imposed on the surface $\eta = \eta_o$. The Leontovich boundary condition can be expressed mathematically as

$$\bar{E} - (\bar{E}\cdot\hat{n})\hat{n} = \tilde{N}\sqrt{\frac{\mu}{\epsilon}}\,(\hat{n}\times\bar{H})\,, \tag{2.26}$$

where $\tilde{N}$ is the relative surface impedance of the walls of the paraboloid (N=0 for the perfectly conducting case). As can be seen from the notation used, the relative

surface impedance is represented as as dyadic function. A nonzero surface impedance has been used for the finite conductivity of waveguides before (see Mohsen and Hamid [1970]). It has also been used to account for the finite conductivity of scatterers (see Senior [1960a]), for the roughness of its surface (Senior [1960b]), and for the presence of highly absorbing coating layers (Weston [1963]).

It should be noted here, that if $\bar{\bar{N}}$ had been assigned a scalar value, this would imply that the impedance is the same in any direction, but this is not the general case. In the more general case considered here, the surface impedance $\bar{\bar{N}}$ is represented by a two dimensional dyadic transforming the tangential components of $\bar{H}$ into the tangential components of $\bar{E}$ on the boundary (see Morse and Feshbach [1953] pp. 1814).

Now substituting Eq. (2.19) and (2.21) into Eq. (2.26) it is found that the Leontovich condition manifests itself in the two equations

$$\frac{E_\xi}{H_\phi} = -N_\xi \sqrt{\frac{\mu}{\epsilon}} \qquad at \quad \eta = \eta_o, \tag{2.27}$$

and

$$\frac{E_\phi}{H_\xi} = N_\phi \sqrt{\frac{\mu}{\epsilon}} \qquad at \quad \eta = \eta_o. \tag{2.28}$$

Substitution of Eq. (2.10) and (2.11) and Eq. (2.14) and (2.15) into Eq. (2.28) and Eq. (2.27) respectively leads to boundary conditions in terms of the potentials given by

$$\frac{\partial U}{\partial \eta} - \frac{i K \sqrt{\xi^2 + \eta^2}}{N_\phi} U = 0 \qquad at \quad \eta = \eta_o ,$$

and

$$\frac{\partial Q}{\partial \eta} - i K N_\xi \sqrt{\xi^2 + \eta^2}\, Q = 0 \qquad at \quad \eta = \eta_o ,$$

which , after performing the differentiation, become

$$U' - \frac{i\sqrt{\xi^2+\eta^2}}{\eta N_\phi} U = 0 \qquad at \quad \eta = \eta_o \ , \tag{2.29}$$

and

$$Q' - \frac{i N_\xi}{\eta}\sqrt{\xi^2+\eta^2}\, Q = 0 \qquad at \quad \eta = \eta_o \ . \tag{2.30}$$

If we assume, for the sake of mathematical simplicity, that

$$N_\phi = -\frac{i}{\eta_o}\sqrt{\xi^2+\eta_o^2} \ , \tag{2.31}$$

and

$$N_\xi = \frac{i\,\eta_o}{\sqrt{\xi^2+\eta_o^2}} \ , \tag{2.32}$$

then the boundary conditions on the potentials simplify to

$$U' + U = 0 \qquad at \quad \eta = \eta_o \ , \tag{2.33}$$

and

$$Q' + Q = 0 \qquad at \quad \eta = \eta_o \ . \tag{2.34}$$

These can be recognized as Dirichlet-Neumann or Robin boundary conditions and can be handled fairly easily by partial differential equation theory.

The physical interpertation of Eq. (2.31) and Eq. (2.34) is that the boundary impedance should vary on the walls of the paraboloid as a function of ξ. The impedance is also reactive since the expressions are totally imaginary. The practical implications and the physical realizability of these boundary conditions will not be considered in any detail.

2.3 Separation of the Partial Differential Equation

Solutions to the partial differential equation given by Eq. (2.13) or Eq. (2.17) must now be found. Since these equations are the same for both potentials $U(\xi,\eta)$ and $Q(\xi,\eta)$ it is sufficient to solve only one of these equations. Thus in the following discussions the U potential will be solved for although the solutions are equally valid for the Q potential. For convenience the equation is rewritten here;

$$\frac{\partial}{\partial \xi}\left(\frac{1}{\rho}\frac{\partial U}{\partial \xi}\right)+\frac{\partial}{\partial \eta}\left(\frac{1}{\rho}\frac{\partial U}{\partial \eta}\right)+\frac{K^2}{\rho}\left(\xi^2+\eta^2\right)U=0\,. \tag{2.13}$$

The method of separation of variables is now undertaken to solve the above equation. Following the general procedure, we assume a solution of the form

$$U(\xi,\eta)=U_1(\xi)U_2(\eta)\,. \tag{2.35}$$

If a separation constant C is chosen, then separation of the equation produces the two ordinary differential equations

$$\frac{d^2}{d\xi^2}U_1(\xi)-\frac{1}{\xi}\frac{d}{d\xi}U_1(\xi)+\left(K^2\xi^2-C\right)U_1(\xi)=0\,, \tag{2.36}$$

and

$$\frac{d^2}{d\eta^2}U_2(\eta)-\frac{1}{\eta}\frac{d}{d\eta}U_2(\eta)+\left(K^2\eta^2+C\right)U_2(\eta)=0\,. \tag{2.37}$$

These equations are identical except for the sign of the parameter C, but since the only restriction on the parameter is that it be a real number, only one of the equations needs be solved. We choose Eq. (2.37), the equation for the variable η, since this equation will provide us with the eigenfunctions in the later chapters. The brute force method could be taken at this point, in that Eq. (2.37) could be solved using the general *method of Frobenius* This elegant method will not be used at the present time but for the sake of completeness and comparison it has been included as

Appendix A at the end of this thesis.

Instead, independent variable transformations will be performed in order to reduce Eq. (2.37) into a form for which a solution is well known. As will soon become apparent, there are a few independent variable transformations which could be used on this differential equation. Three reduced forms will be presented. The third form is the one which will be used and advantages of this form will become apparent when compared to the others.

As a first independent variable transformation we let

$$y(x) = y(iK\eta^2) = U_2(\eta), \tag{2.38}$$

where

$$x = iK\eta^2. \tag{2.39}$$

From these transformations the differentials with respect to x can be expressed as

$$\frac{d}{d\eta} = 2iK\eta\frac{d}{dx}$$

$$\frac{d^2}{d\eta^2} = -4K^2\eta^2\frac{d^2}{dx^2} + 2iK\frac{d}{dx}$$

and these when substituted into Eq. (2.37) transform that equation into

$$\frac{d^2}{dx^2}y(x) + \left[\frac{-1}{4} + \frac{iC}{4Kx}\right]y(x) = 0. \tag{2.40}$$

This equation can be recognized as Whittaker's standard differential equation (see Erdelyi et.al. [1953], Abramowitz and Stegun [1965]) which takes the form

$$\frac{d^2}{dx^2}w(x) + \left[\frac{-1}{4} + \frac{k}{x} + \frac{1/4-\mu^2}{x^2}\right]w(x) = 0, \tag{2.41}$$

where for our case

$$w(x) = y(x), \quad \mu = \frac{1}{2} \quad \text{and} \quad k = \frac{iC}{4K}.$$

The Whittaker equation can be derived from the more general confluent hypergeometric equation

$$x \frac{d^2}{dx^2} v(x) + (b - x) \frac{d}{dx} v(x) - a\, v(x) = 0 \tag{2.42}$$

by the transformation

$$v(x) = x^{-b/2} e^{x/2} w(x), \quad a = \frac{1}{2} - k + \mu, \quad b = 1 + 2\mu,$$

where for our case

$$y(x) = x\, e^{-x/2} v(x), \quad a = 1 - \frac{iC}{4K} \quad \text{and} \quad b = 2.$$

Solutions to Eq. (2.42) are denoted as (see Abramowitz and Stegun [1965]),

$$M(a, b, x) \quad \text{and} \quad U(a, b, x),$$

and are called Kummer's functions.

Solutions to the potentials could be arrived at through the solution of either Eq. (2.41) or Eq. (2.42). Both of these forms were derived from the original differential equation and are perfectly valid but are awkward to use because of the complex transformation which was required to obtain them. Not only is the variable a complex transformation of the original but the new parameter would also be a complex number. This parameter would ultimately become our eigenvalue and would thus be prefered to be real. Given these problems, alternate forms of Eq. (2.37) are sought.

2.3.1 Alternate Transformation ; Coulomb Wave Equation

If instead of the transformation defined by Eq. (2.38) we use the transformation

$$z = \frac{1}{2} K \eta^2 \; ; \; y(z) = U_2(\frac{1}{2} K \eta^2) \, , \tag{2.43}$$

then the differentials with respect to z become

$$\frac{d}{d\eta} = K \eta \frac{d}{dz}$$

and

$$\frac{d^2}{d\eta^2} = K^2 \eta^2 \frac{d^2}{dz^2} + K \frac{d}{dz} \, .$$

Therefore substitution of these into Eq. (2.37) reduces that equation into

$$\frac{d^2}{dz^2} y(z) + \left[1 + \frac{C}{2Kz} \right] y(z) = 0 \, , \tag{2.44a}$$

or

$$\frac{d^2}{dz^2} y(z) + \left[1 + \frac{2\lambda}{z} \right] y(z) = 0 \, , \tag{2.44b}$$

where

$$\lambda = \frac{C}{4K} \, .$$

This can be recognized as the Coulomb wave equation of order L=0

$$\frac{d^2}{dz^2} y(z) + \left[1 - \frac{2\beta}{z} - \frac{L(L+1)}{z^2} \right] y(z) = 0 \, , \tag{2.45}$$

where for the present case

$$\beta = -\lambda = -\frac{C}{4K} . \tag{2.46}$$

The Coulomb wave equation has a regular singularity at the point z=0 and an irregular singularity at z=∞ . The general solution of Eq. (2.45) is

$$y(z) = C_1 F_l(\beta, z) + C_2 G_l(\beta, z) , \tag{2.47}$$

where C_1 and C_2 are constants. For the specific case of Eq. (2.44) the solution can be written as

$$y(z) = C_1 F_0(\beta, z) + C_2 G_0(\beta, z) , \tag{2.48}$$

where β is given by Eq. (2.46). The reason for introducing the negative sign in front of λ is that when we define Eq. (2.44) as a Sturm-Liouville system it will prove to be more convenient, since λ will be defined as the eigenvalue.

It should be noted at this time that the Coulomb wave equation can be derived from the confluent hypergeometric equation by the transformation

$$F_L(\beta, z) = e^{-iz} z^{L+1} C_L(\beta) M(L+1-i\beta, 2L+2, 2iz) , \tag{2.49}$$

where

$$C_L(\beta) = 2^L e^{\frac{-\pi\beta}{2}} \frac{|\Gamma(L+1-i\beta)|}{\Gamma(2L+2)} . \tag{2.50}$$

Of the three forms of Eq. (2.37), the Coulomb wave equation [Eq. (2.45)] will be used in the following chapters as the form to be solved. Thus in the next chapter the mathematical properties of the solutions to this equation will be investigated. As well the numerical algorithms for the computation of these functions will be examined.

CHAPTER 3

THE COULOMB WAVE FUNCTIONS

In this chapter the mathematical properties of the Coulomb wave equation and its solution, the Coulomb wave functions, will be investigated. These functions will be investigated in the form of a Sturm-Liouville system since the ultimate goal for their use is as eigenfunctions for the solution of rotationally symmetric electromagnetic fields inside the rotation-paraboloidal waveguide. Numerical results will also be presented at the end of this chapter. These will include numerical tabulations and graphs of the wave functions as well as graphs of the eigenfunctions for the Dirichlet, Neumann and Impedance boundary condition cases.

3.1 Sturm-Liouville Systems

The notation which will be used in the following discussion for a regular Sturm-Liouville system follows that of Trim [1986], and is shown below :

$$\left[r(z)y'(\lambda,z)\right]' + \left[\lambda p(z) - q(z)\right]y(\lambda,z) = 0, \quad a < z < b, \tag{3.1a}$$

$$-l_1 y'(\lambda,a) + h_1 y(\lambda,a) = 0, \tag{3.1b}$$

$$l_2 y'(\lambda,b) + h_2 y(\lambda,b) = 0. \tag{3.1c}$$

The constants h_1, h_2, l_1, and l_2 in the Robin boundary conditions are real and independent of the parameter λ. The functions $p(z)$, $q(z)$, $r(z)$, and $r'(z)$ are real and continuous over the specified interval. Also, it is assumed that $p(z) > 0$ and $r(z) > 0$ for $a < z < b$. The parameter λ takes on a denumerably infinite set of values λ_n (n = 1,2, ...) for which the corresponding non-trivial solution of Eq. (3.1) is denoted

$$y_n(z) = y(\lambda_n, z).$$

The $y_n(z)$ are called the eigenfunctions of the Sturm-Liouville system and λ_n are the eigenvalues.

3.1.2 The Coulomb Wave Functions as a Sturm-Liouville System

For the case of the Coulomb wave functions and the rotation-paraboloidal coordinates the specific values of the functions in the system of Eq. (3.1) are provided from Eq. (2.44b) where

$$r(z) = 1.0\,,\ p(z) = \frac{2}{z}\,,\ \text{and}\ q(z) = -1.0\,,$$

where the range of the variable z is $0 < z < z_o$. It is noted that r, p, and q satisfy all of the necessary requirements quoted above. For the case of the paraboloidal waveguide there will be no boundary condition at $z = 0$, but only at $z = z_o$ (ie. the walls of the paraboloidal waveguide). Thus the singular Sturm-Liouville system

$$y_n''(z) + \left[1 + \lambda_n \left(\frac{2}{z}\right)\right] y_n(z) = 0\,, \qquad 0 < z < z_o\,, \tag{3.2a}$$

$$l_2 y_n'(z_o) + h_2 y_n(z_o) = 0\,, \tag{3.2b}$$

arises, where at least one of l_2 and h_2 is not equal to zero. If $l_2 = 0$ we have a Dirichlet condition at $z = z_o$. If $h_2 = 0$ we have a Neumann condition at $z = z_o$. If both l_2 and h_2 exist then we have a Robin condition at $z = z_o$, which will be necessary for the impedance boundary condition case as explained in Sec. 2.2.2. Thus it will be necessary to obtain numerical results for all three cases.

The above system of Eq. (3.2) is a singular Sturm-Liouville system since only one boundary condition exists. Thus the general properties of a regular Sturm-Liouville system cannot be used without proof. One of the most useful of these properties which will be required in later discussions is the orthogonality of the

eigenfunctions with respect to the weighting function $p\,(z)$.

Consider the eigenvalue-eigenfunction pairs $\left\{y_m, \lambda_m\right\}$ and $\left\{y_n, \lambda_n\right\}$. The differential equation satisfied by each of these eigenvalue-eigenfunction pairs is given by Eq. (3.2a)

$$y_n''(z) + \left[1 + \lambda_n \left(\frac{2}{z}\right)\right] y_n(z) = 0\,, \quad 0 < z < z_o\,, \tag{3.3a}$$

$$y_m''(z) + \left[1 + \lambda_m \left(\frac{2}{z}\right)\right] y_m(z) = 0\,, \quad 0 < z < z_o\,. \tag{3.3b}$$

The following manipulations are now performed :

$$y_m \left\{y_n''(z) + \left[1 + \lambda_n \left(\frac{2}{z}\right)\right] y_n(z)\right\} -$$

$$y_n \left\{y_m''(z) + \left[1 + \lambda_m \left(\frac{2}{z}\right)\right] y_m(z)\right\} = 0\,,$$

$$y_m y_n'' - y_n y_m'' = y_n y_m \left(\lambda_m - \lambda_n\right) \frac{2}{z} = \left(y_m y_n'\right)' - \left(y_n y_m'\right)'.$$

Integrating with respect to z over the interval, we get

$$\left(\lambda_m - \lambda_n\right) \int_0^{z_o} y_m y_n \left(\frac{2}{z}\right) dz = \begin{vmatrix} y_m(z_o) & y_m'(z_o) \\ y_n(z_o) & y_n'(z_o) \end{vmatrix} - \begin{vmatrix} y_m(0) & y_m'(0) \\ y_n(0) & y_n'(0) \end{vmatrix}.$$

Now for orthogonality of the eigenfunctions with respect to the weighting function p(z), the right side of the above equation must be equal to zero. The first determinant is equal to zero because of the existence of the boundary condition at $z = z_o$. That is, if one thinks of the boundary equations at $z = z_o$ for y_m and y_n as simultaneouse equations in l_2 and h_2, then since these equations have nontrivial solutions (ie. at least one of l_2 and h_2 must exist) the determinant must go to zero.

The second determinant will not collapse to zero as easily as the first because there is no boundary condition at z=0. We will find that if we examine the properties of the solutions of the of the Coulomb wave equation we will see that one of the solutions is identically zero at z=0. Thus this solution will be orthogonal. As will be seen in later discussions, the second solution will not be appropriate and thus will not be used in the eigenfunction solution because it produces a singularity in the field at z=0. Therefore the orthogonality of the second solution is not required.

Now that we have established orthogonality it is convenient to normalize the eigenfunctions. Thus a normalization constant N, can be defined by

$$N^2 = \int_0^{z_e} y_m y_n \left(\frac{2}{z}\right) dz \ . \tag{3.4}$$

The eigenfunctions will be divided by N in order to make them orthonormal.

3.2 Properties of the Coulomb Wave Functions

In this section the properties of the Coulomb wave functions will be investigated. These properties are results obtained from many authors over a number of years (see National Bureau of Standards [1952], Fröberg [1955], Luk'Yanov et.al. [1965]). The notation which will be used here is that of Abramowitz and Stegun [1972], which was a compilation of the properties known about the functions up until the year 1965. The results which will be shown here will be modified to the case where L=0 so that they can be directly applied to the problem at hand.

The solution of the Coulomb wave equation [Eq. (2.45)], consists of the two solutions given in Eq. (2.47). In the following discussions the parameter β will be used, where β is related to λ by Eq. (2.46). The solution $F_0(\beta, z)$ is called the regular Coulomb wave function while $G_0(\beta, z)$ is called the irregular or logarithmic Coulomb wave function.

3.2.1 The Regular Wave Function

The regular Coulomb wave function can be expressed in terms of the confluent hypergeometric equation, as mentioned in the previous chapter, as

$$F_0(\beta, z) = C_0(\beta) z\, e^{-iz} M(1 - i\beta, 2, 2iz),$$

where

$$C_0(\beta) = \left[\frac{2\pi\beta}{(e^{\pi\beta} - 1)}\right]^{\frac{1}{2}}. \tag{3.5}$$

A more appropriate form for numerical computations is

$$F_0(\beta, z) = C_0(\beta) z\, \Phi_0(\beta, z), \tag{3.6}$$

where

$$\Phi_0(\beta, z) = \sum_{n=1}^{\infty} A_n(\beta) z^{n-1}, \tag{3.7}$$

and

$$A_1 = 1, \; A_2 = \beta, \; n(n-1)A_n = 2\beta A_{n-1} - A_{n-2} \quad (n > 2). \tag{3.8}$$

The asymptotic theory of linear difference equations shows that this equation is stable (i.e. a small change in the parameter β will cause only a small change in the A_n for large n). For an analysis of this point the reader is referred to appendix B.

The derivative with respect to z of the regular wave function can be computed by the relation

$$F_0' = \frac{d}{dz} F_0 = C_0(\beta) \Phi_0^*(\beta, z), \tag{3.9}$$

where

$$\Phi_0^* = \sum_{n=1}^{\infty} n A_n(\beta) z^{n-1} . \tag{3.10}$$

The above series relations were used to compute the regular wave function for $0 < z < 5$, and for the parameter β ranging from +5 to -10. The results were checked with published results such as those of the National Bureau of Standards [1952] and Luk'Yanov et.al. [1965]. The only source found for negative values of β was the National Bureau of Standards [1952]. The reason for the scarcity of results in this region is probably due to the fact that negative values of β have no physical significance in the use of these functions to express the Coulomb field about a nucleus.

Unfortunately the series representations given above cannot be used for all values of z and β. For different regions in the $z-\beta$ plane different methods of computation must be used (see Fröberg [1955]). One important region in this plane is called the transition region or the turning points where $z = 2\beta$. Asymptotic expansions for $z = 2\beta > 0$ are given by

$$F_0(2\beta) = .7063326373\,\beta^{1/6} \times$$

$$\left[1 - \frac{.04959570165}{\beta^{4/3}} - \frac{.00888888889}{\beta^2} - \frac{.002455199181}{\beta^{10/3}} - \ldots\right], \tag{3.11}$$

and

$$F_0'(2\beta) = .4086957323\,\beta^{-1/6} \times$$

$$\left[1 + \frac{.1728260369}{\beta^{2/3}} + \frac{.0003174603174}{\beta^2} + \frac{.003581214850}{\beta^{8/3}} + \ldots\right]. \tag{3.12}$$

For values of z where the series solution was inacurate the values of the function and its derivative at the turning points was used as initial values and the differential equation was integrated using the Runge-Kutta-Verner fifth and sixth

order method. The algorithm which was used was from the International Mathematical and Statistical Library [1982]. Calculations were performed for values of z down from the turning points and up from the turning points with a relative accuracy of 10^{-5}. Plots of the regular Coulomb wave function and its derivative are shown in Fig. 3.1 and Fig. 3.2 respectively.

As can be seen from the graphs, at the point z=0 the regular coulomb wave function takes on the value

$$F_0(\beta,0) = 0\,, \tag{3.13}$$

while, not so obviousely, its derivative takes on the value

$$F_0'(\beta,0) = C_o(\beta)\,. \tag{3.14}$$

3.2.2 The Irregular Wave Function

The irregular or logarithmic Coulomb wave function can be expressed in terms of the regular wave function as

$$G_0(\beta,z) = \frac{2\beta}{C_0^2(\beta)} F_0(\beta,z)\left[\ln(2z) + \frac{q_0(\beta)}{p_0(\beta)}\right] + \Theta_0(\beta,z)\,, \tag{3.15}$$

where

$$\Theta_0(\beta,z) = \frac{\psi_0(\beta,z)}{C_0(\beta)}\,, \tag{3.16}$$

and

$$\psi_0(\beta,z) = \sum_{n=0}^{\infty} a_n(\beta) z^n\,,$$

$$a_0 = 1\,,\ a_1 = 0\,,\ n(n-1)a_n = 2\beta a_{n-1} - a_{n-2} - (2n-1)2\beta A_n\,, \tag{3.17}$$

where A_n is the same coefficient as that used in the series expansion of the regular

wave function given in Eq. (3.8) and $C_0(\beta)$ is given by Eq. (3.5). Also we have

$$\frac{q_0(\beta)}{p_0(\beta)} = -1 + Real\left\{\frac{\Gamma'(1+i\beta)}{\Gamma(1+i\beta)}\right\} + 2\gamma$$

$$= -1 + \gamma + \beta^2 \sum_{n=1}^{\infty} \frac{1}{n\,(n^2+\beta^2)}\,, \tag{3.18}$$

where γ is Euler's number , γ = .577215665.

Unlike the series representation for the regular Coulomb wave function, the above representation is very difficult to compute by. Thus the differential equation was integrated using the same Runge-Kutta method as for the regular wave function. The initial values used were also the values of the function and its derivative at the turning points, which are given by

$$G_0(2\beta) = 1.223404016\,\beta^{1/6} \times$$

$$\left[1 + \frac{.04959570165}{\beta^{4/3}} - \frac{.00888888889}{\beta^2} + \frac{.002455199181}{\beta^{10/3}} - \ldots\right], \tag{3.19}$$

and

$$G_0'(2\beta) = -.7078817734\,\beta^{-1/6} \times$$

$$\left[1 - \frac{.1728260369}{\beta^{2/3}} + \frac{.0003174603174}{\beta^2} - \frac{.003581214850}{\beta^{8/3}} + \ldots\right]. \tag{3.20}$$

The irregular wave functions were calculated for the same ranges as for the regular wave functions and the plots are shown in Fig. 3.3 and Fig. 3.4.

At the point z=0 the irregular wave function can be determined from

$$G_0(\beta,0) = \frac{1}{C_0(\beta)}\,, \tag{3.21}$$

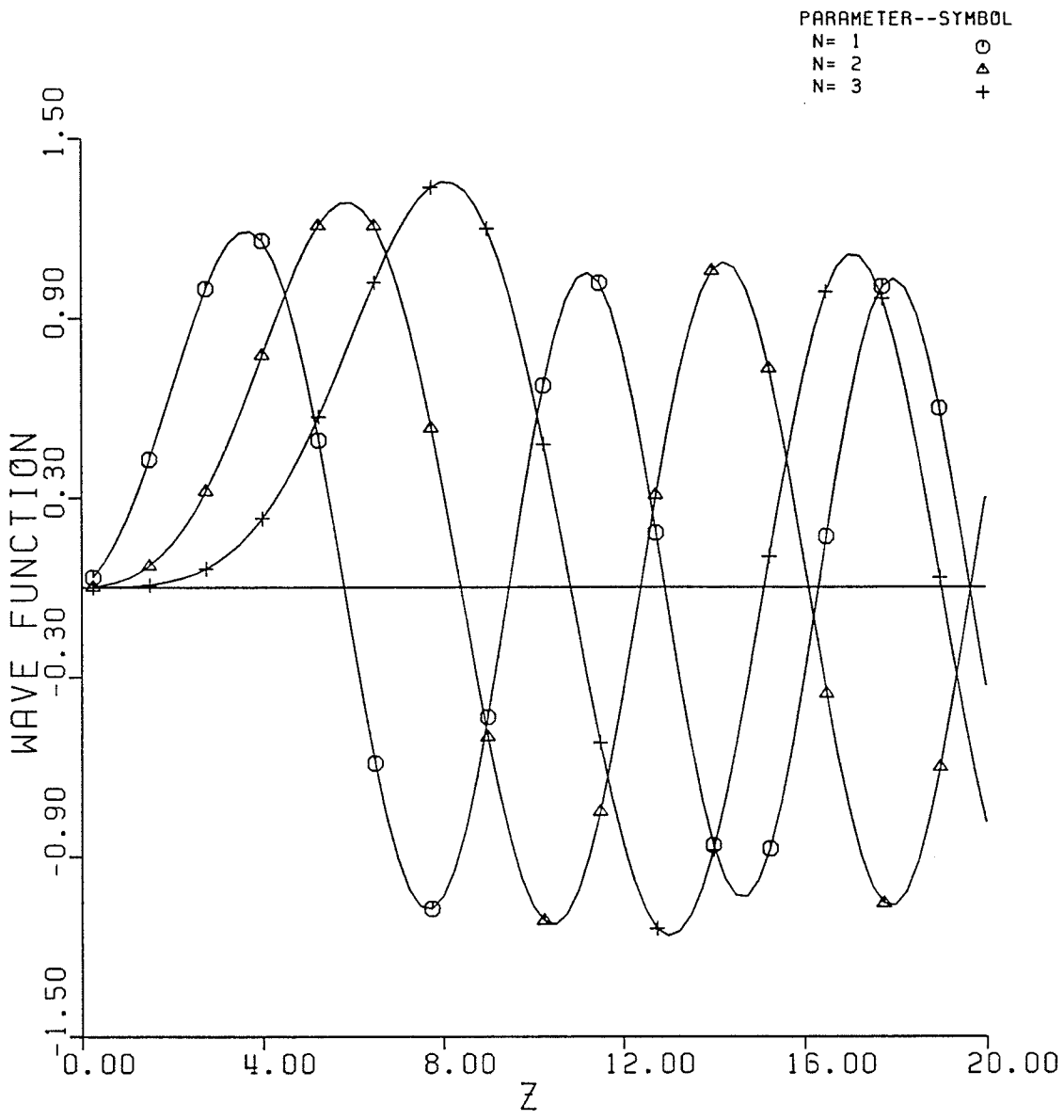
REGULAR COULOMB WAVE
FUNCTION F(N,Z)
PARAMETER--SYMBOL
N= 1
N= 2
N= 3
WAVE FUNCTION
1.50
0.90
0.30
-0.30
-0.90
-1.50
0.00
4.00
8.00
12.00
16.00
20.00
Z

FIGURE 3.1

DERIVATIVE OF REGULAR COULOMB WAVE FUNCTION F(N, Z)

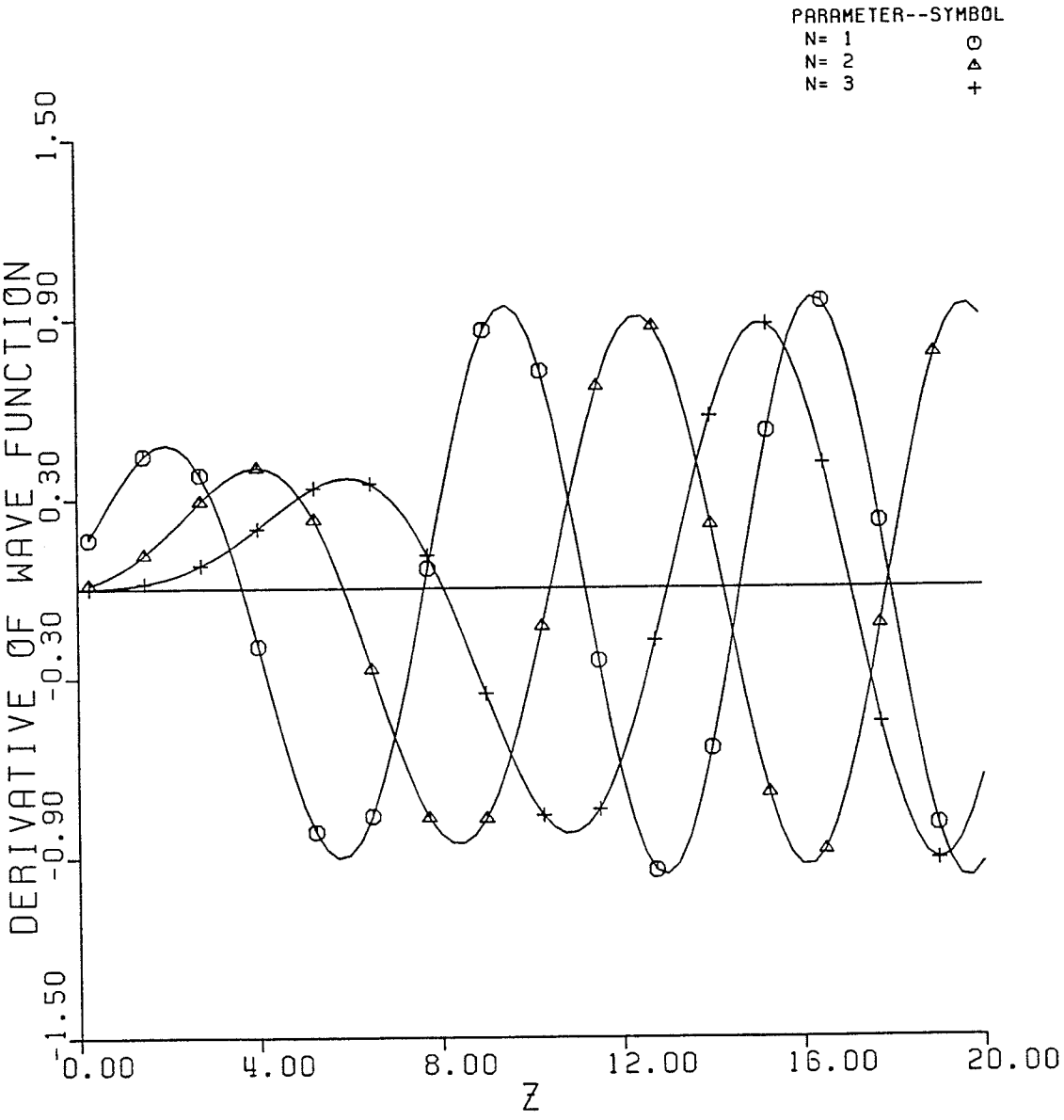

FIGURE 3.2

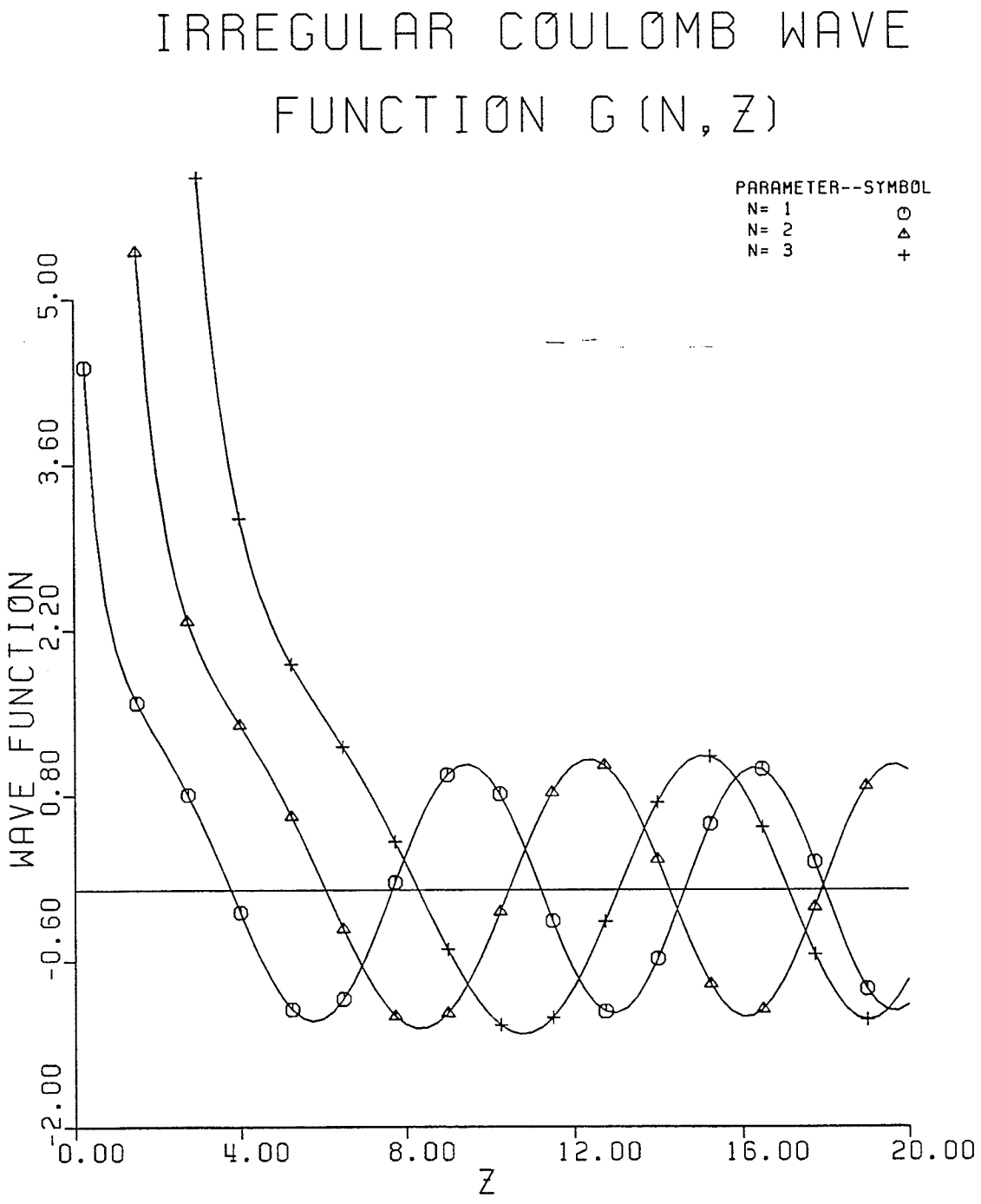
IRREGULAR COULOMB WAVE
FUNCTION G(N, Z)
PARAMETER--SYMBOL
N= 1
N= 2
N= 3
WAVE FUNCTION
5.00
3.60
2.20
0.80
-0.60
-2.00
0.00
4.00
8.00
12.00
16.00
20.00
Z

FIGURE 3.3

DERIVATIVE OF IRREGULAR COULOMB WAVE FUNCTION G(N,Z)

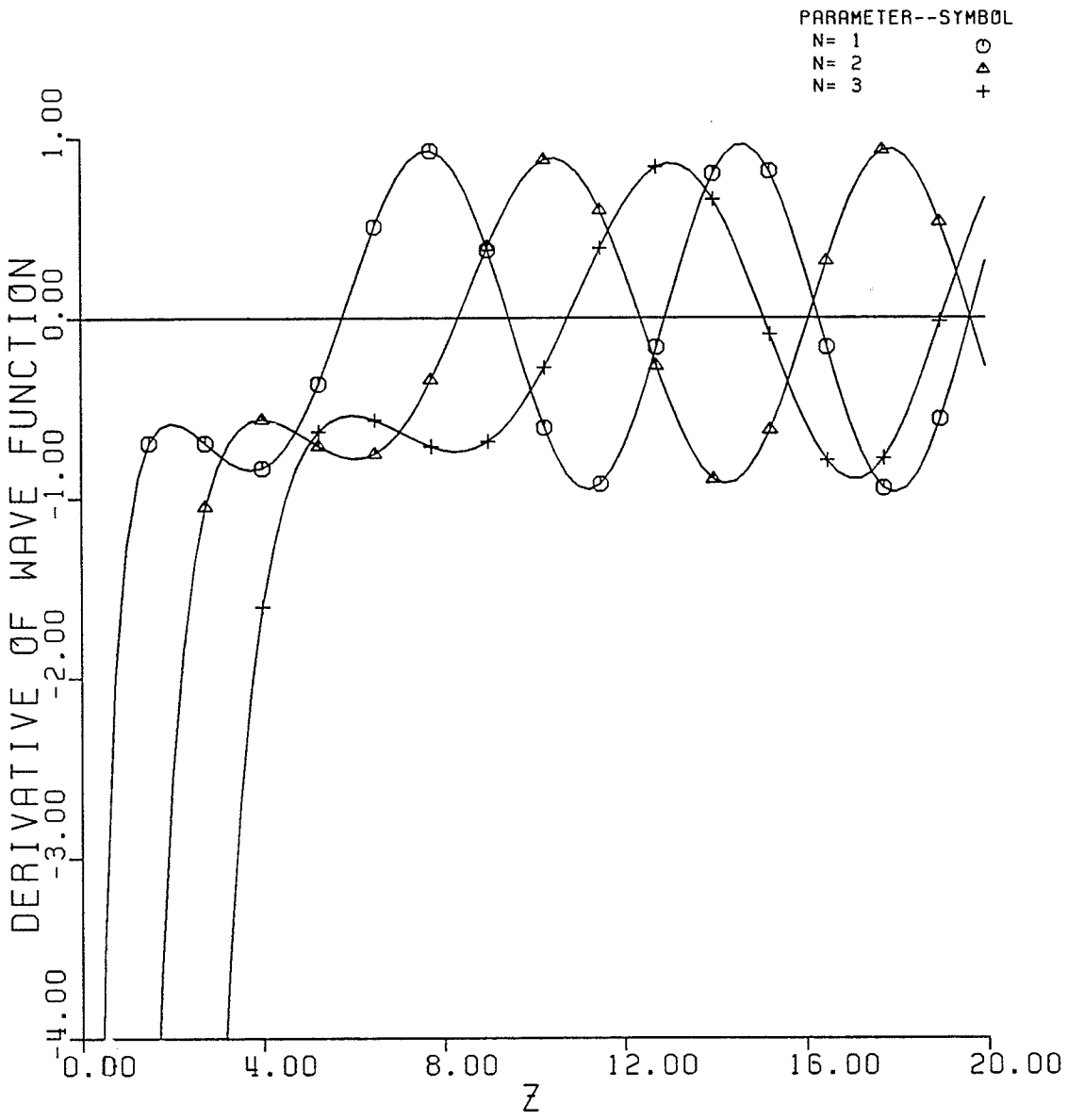

FIGURE 3.4

and its derivative from

$$G_0'(\beta,0) = -\infty \ . \tag{3.22}$$

3.2.3 Wave Functions of the Third Kind

The two solutions $F_0(\beta,z)$ and $G_0(\beta,z)$ can be combined to form two alternate solutions which we shall call Coulomb wave functions of the third kind. These new functions are defined as

$$H_0^1(\beta,z) = G_0(\beta,z) + iF_0(\beta,z)\,, \tag{3.23}$$

and

$$H_0^2(\beta,z) = G_0(\beta,z) - iF_0(\beta,z)\,. \tag{3.24}$$

These functions are useful in terms of their asymptotic representations for large z, for as z gets large

$$H_0^1(\beta,z) \to e^{i\theta_0}\,, \tag{3.25}$$

and

$$H_0^2(\beta,z) \to e^{-i\theta_0}\,, \tag{3.26}$$

where

$$\theta_0 = z - \beta\ln(2z) + arg\left\{\Gamma(1+i\beta)\right\}. \tag{3.27}$$

These functions and the method of defining them are analogous to the exponential expansions of the Hankel functions which are defined in a similar way but should not be confused with the above functions.

3.3 Solutions for the Potentials

Now that we have solutions to the basic differential equation, the solutions for the Abraham potentials $U(\xi,\eta)$ and $Q(\xi,\eta)$ can be constructed using these solutions. The eigenfunctions will be represented by the regular Coulomb wave functions $F_0(-\lambda_n, \tfrac{1}{2}K\eta^2)$ with the eigenvalues λ_n appropriately chosen in order that the boundary conditions at $\eta = \eta_o$ will be satisfied. These boundary conditions can be either Dirichlet, Neumann, or Robin boundary conditions, whichever are required, as explained in the previous chapter. The irregular Coulomb wave functions are not used as eigenfunctions because, not only are they not orthogonal, but from Eq. (2.10) and Eq. (2.14) they would produce a singularity in the field at $\eta = 0$ (i.e. the axis of the paraboloid). The regular wave functions do not produce such singularity since they produce a zero over zero term and L'Hopital's rule can be used to take the limit as η goes to 0. This limit turns out to be finite and thus there is no singularity.

In the ξ coordinate the functions which will be used are $F_0(\lambda, \tfrac{1}{2}K\xi^2)$ for regions including the $\xi = 0$ axis and $H_0^1(\lambda, \tfrac{1}{2}K\xi^2)$ for regions not including the $\xi = 0$ axis. The reason that H_0^1 is chosen is clear from Eq. (3.25) and the $e^{-i\omega t}$ time dependence since these functions would best describe outward travelling waves. Thus the potentials can be constructed as

$$U(\xi,\eta) = \begin{cases} \sum_n A_n F_0\left(\lambda_n, \frac{1}{2}K\xi^2\right) F_0\left(-\lambda_n, \frac{1}{2}K\eta^2\right) & 0 < \eta < \eta_o \text{ , } \xi = 0 \textit{ region} \text{ ,} \\ \sum_n B_n H_0^1\left(\lambda_n, \frac{1}{2}K\xi^2\right) F_0\left(-\lambda_n, \frac{1}{2}K\eta^2\right) & 0 < \eta < \eta_o \text{ , } \xi = \textit{large region} \text{ ,} \end{cases} \tag{3.28}$$

and

waveguide.

The transcendental equation which arises from applying the Dirichlet condition to U is obtained by applying Eq. (2.25) to Eq. (3.28) and can be simply written as

$$F_0(-\lambda_n, \frac{1}{2}K\eta_o^2) = 0. \tag{3.30}$$

Thus all values of λ_n which satisfy this equation are the eigenvalues. The regular Coulomb wave function has been plotted as a function of the parameter λ_n (shown as N in the plot) and is shown in Fig. 3.5. The three frequencies 100, 250 and 500 MHz were chosen with a constant coordinate η_o of the paraboloid corresponding to a focal length of 1 meter. The zero crossings, which are the eigenvalues, were then obtained by a numerical technique and the first few eigenvalues are shown in Table 3.1 for the respective frequencies.

$$Q(\xi,\eta) = \begin{cases} \sum_n A_n F_0\left(\lambda_n, \frac{1}{2}K\xi^2\right) F_0\left(-\lambda_n, \frac{1}{2}K\eta^2\right) & 0 < \eta < \eta_o \ , \ \xi = 0 \ region \\ \sum_n B_n H_0^1\left(\lambda_n, \frac{1}{2}K\xi^2\right) F_0\left(-\lambda_n, \frac{1}{2}K\eta^2\right) & 0 < \eta < \eta_o \ , \ \xi = large \ region \ . \end{cases} \tag{3.29}$$

The summation over n in the above equations represents a summation over the ordered eigenvalues where the eigenvalues $\lambda_n = C_n / 4K$ are obtained from the transcendental equation produced by applying the boundary conditions on the walls of the waveguide. Eigenvalues for all three types of boundary conditions will be given in the next section.

3.4 Eigenvalues

As discussed in Sec. 2.2 the application of specific boundary conditions to the field at $\eta = \eta_o$ will result in specific boundary conditions for the potential U and Q. These boundary conditions will determine the appropriate eigenvalues for the problem under consideration. From Sturm-Lioville system theory we know that there is a denumerably infinite number of eigenvalues which can be ordered according to ascending value (see Mackie [1965] or Trim [1986]). It is also known, and is quite obvious from the preceding statement, that all the eigenvalues are positive in value except for a finite amount of them (i.e. not an infinite amount). The three cases of Sec. 2.2 will now be considered. The first few eigenvalues will be calculated for all three cases along with the normalization constants N. Of course N will be different for each eigenvalue.

3.4.1 Perfectly Conducting Case

If the paraboloidal waveguide is perfectly conducting, or can at least be assumed to be perfectly conducting, then the Dirichlet condition arises for the potential $U(\xi,\eta)$ and the Neumann condition arises for the potential $Q(\xi,\eta)$. Recall that the potential U represents circularly symmetric T.E. modes and the potential Q represents circularly symmetric T.M. modes inside the paraboloidal

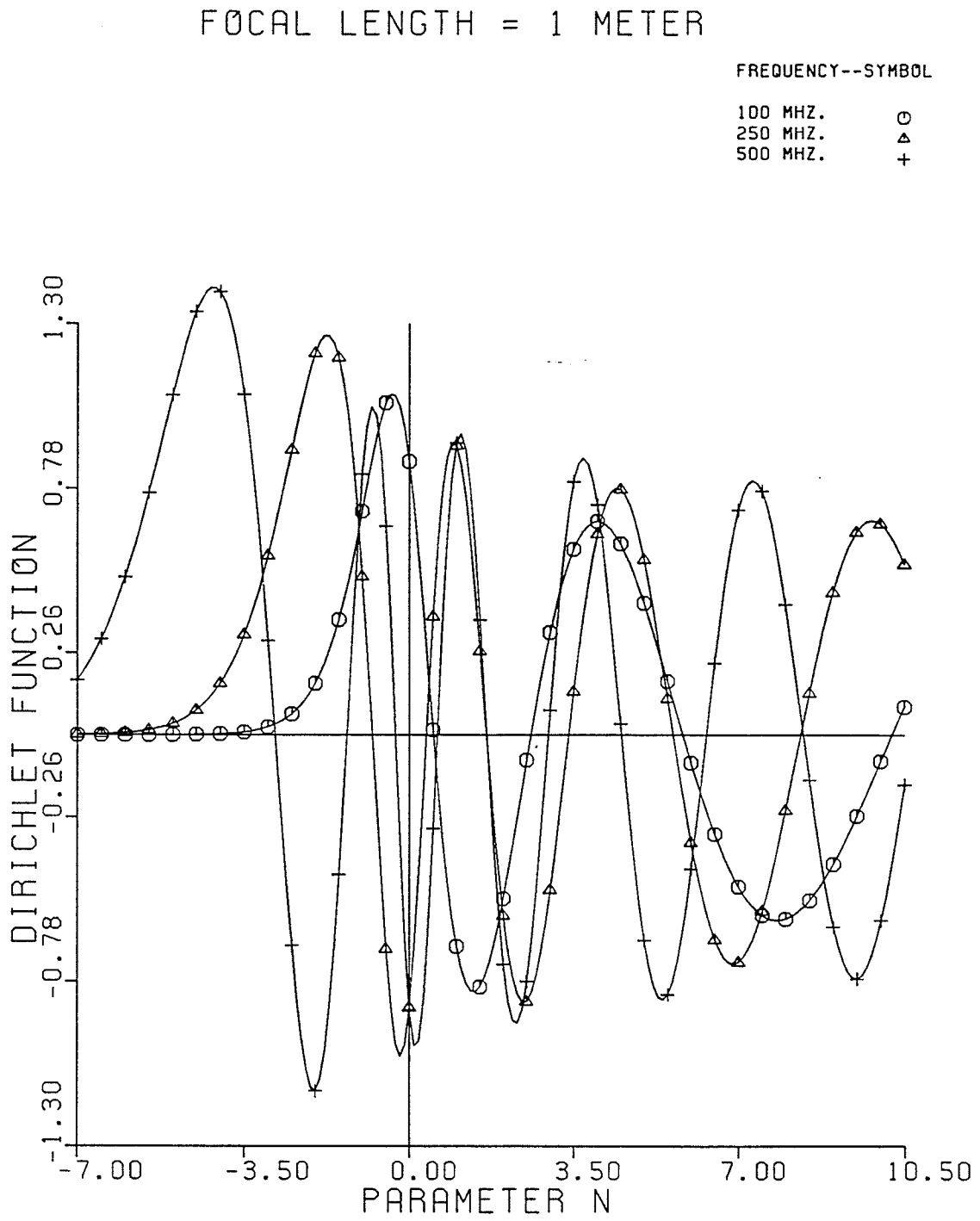

FIG. 3.5: DIRICHLET BOUNDARY FUNCTION

TABLE 3.1						
Eigenvalues and Normalization Constant for the Dirichlet Case						
Focal Length = 1 meter						
Freq.	100MHz		250MHz		500MHz	
n	λ_n	N	λ_n	N	λ_n	N
1	0.5083	1.4072	-0.7868	1.5105	-2.8482	1.2835
2	2.5904	1.0893	0.3574	1.6910	-1.3326	1.6026
3	5.8261	0.9063	1.6424	1.4426	-0.2952	1.8698
4	10.240	0.7925	3.3919	1.2568	0.5911	1.8304
5			5.6191	1.1289	1.6480	1.6289
6			8.3209	1.0340	2.9597	1.4781
7					4.5213	1.3657
8					6.3269	1.2770
9					8.3735	1.2043

For the Neumann condition the transcendental equation which arises can be obtained by applying Eq. (2.24) to Eq. (3.29) and can be written as

$$F_0'(-\lambda_n, \frac{1}{2}K\eta_o^2) = 0. \tag{3.31}$$

This function has also been plotted as a function of the parameter λ_n (also shown as N in the plot) and is shown in Fig. 3.6. The same frequencies and size of the paraboloid were chosen as for the Dirichlet case. The eigenvalues with the respective normalization constants are shown in Table 3.2.

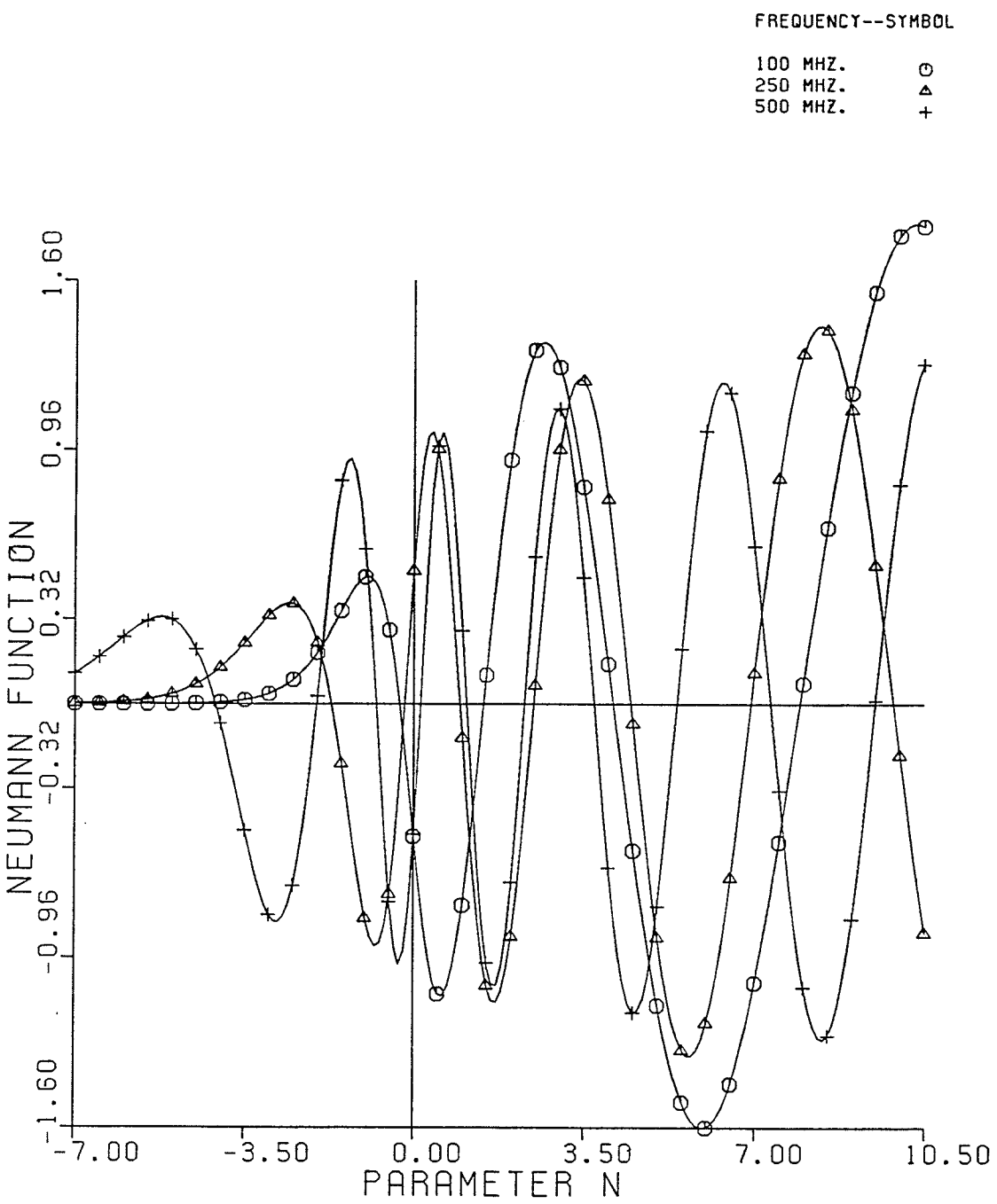

FIG. 3.6: NEUMANN BOUNDARY FUNCTION

TABLE 3.2						
Eigenvalues and Normalization Constant for the Neumann Case						
Focal Length = 1 meter						
Freq.	100MHz		250MHz		500MHz	
n	λ_n	N	λ_n	N	λ_n	N
1	-0.2853	1.2951	-1.7051	1.1140	-4.1067	0.9635
2	1.4408	1.2257	-0.1828	1.6856	-2.0163	1.4433
3	4.1050	0.9839	0.9510	1.5658	-0.7743	1.7475
4	7.9360	0.8433	2.4663	1.3383	0.1426	1.8993
5			4.4589	1.1868	1.0895	1.7245
6			6.9264	1.0779	2.2746	1.5466
7			9.8667	0.9945	3.7134	1.4177
8					5.3987	1.3186
9					7.3261	1.2387
10					9.4931	1.1722

3.4.2 Non-perfectly Conducting Case

For the case where the walls are non-perfectly conducting or absorbing, the Robin condition arises for both potentials if we assume the wall impedances to be given by Eq. (2.31) and Eq. (2.32). The transcendental equation is derived by applying Eq. (2.33) or (2.34) to Eq. (3.28) or (3.29). This transcendental equation can be written as

$$F_0'(-\lambda_n, \frac{1}{2}K\eta_o^2) + F_0(-\lambda_n, \frac{1}{2}K\eta_o^2) = 0. \qquad (3.32)$$

This function, here called the Robin function, is plotted as a function of the parameter λ_n (shown as N in the plot) and is shown in Fig. 3.7. The zero crossings represent the eigenvalues, and these were found along with the normalization constants for the same frequencies and size of paraboloid as for the previous two cases. The eigenvalues and normalization constants for the range of the parameter shown in Fig. 3.7 are tabulated in Table 3.3.

TABLE 3.3

Eigenvalues and Normalization Constant for the Robin Case

Focal Length = 1 meter

Freq.	100MHz		250MHz		500MHz	
n	λ_n	N	λ_n	N	λ_n	N
1	0.1161	1.4991	-1.1043	1.4409	-3.2193	1.2492
2	1.8132	1.2051	0.0852	1.7392	-1.6168	1.5560
3	4.5313	0.9782	1.2410	1.5298	-0.5186	1.8323
4	8.3900	0.8414	2.8113	1.3210	0.3580	1.8864
5			4.8424	1.1784	1.3408	1.6894
6			7.3367	1.0734	2.5666	1.5256
7			10.2960	0.9920	4.0379	1.4048
8					5.7492	1.3102
9					7.6977	1.2330
10					9.8820	1.1682

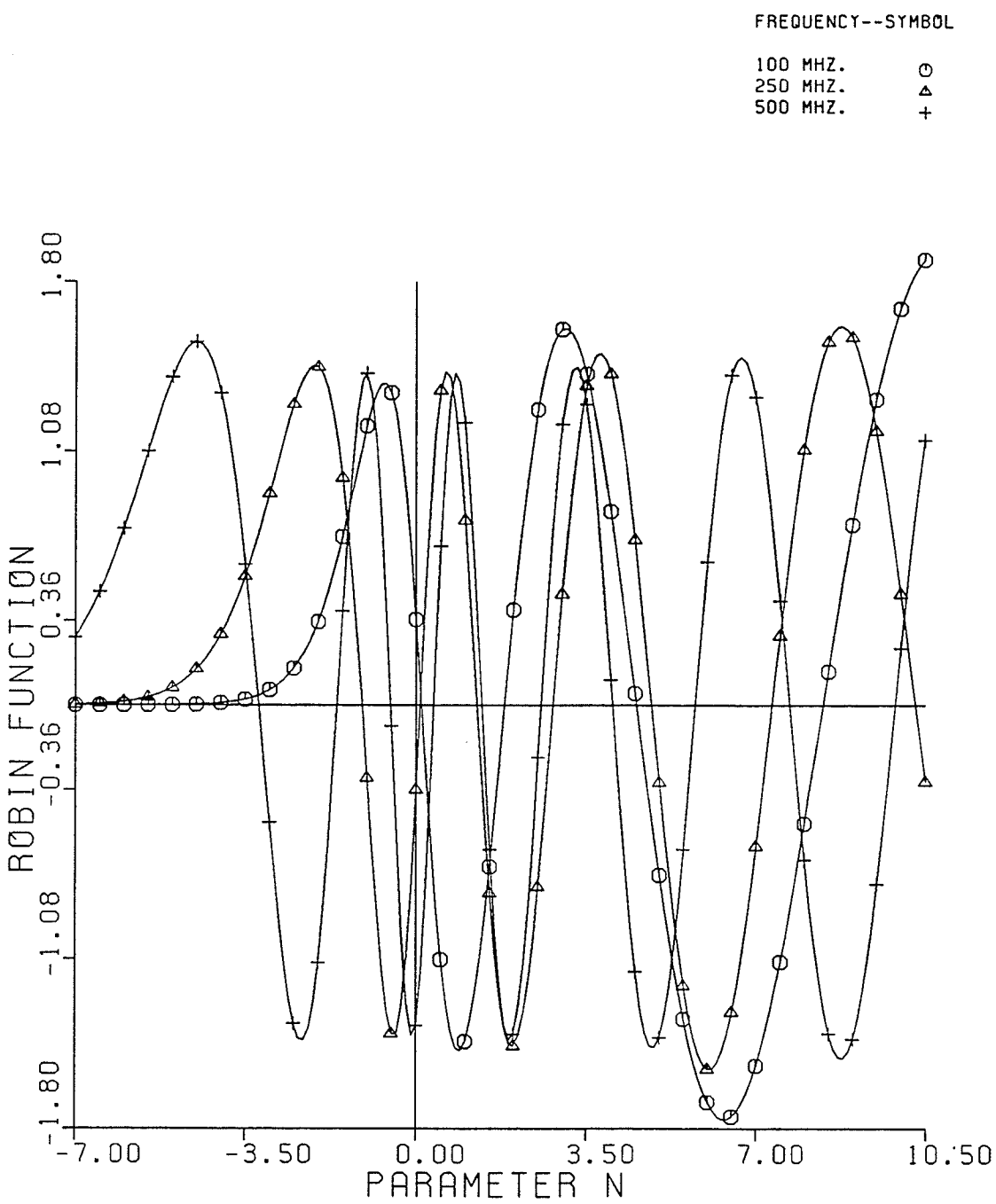

FIG. 3.7: ROBIN BOUNDARY FUNCTION

3.5 Eigenfunctions and Fields

The eigenfunctions for the potentials $U(\xi,\eta)$ and $Q(\xi,\eta)$ are given by the regular Coulomb wave functions with the parameter equal to the negative of the eigenvalue, $-\lambda_n$. These eigenfunctions are then normalized by the normalization constant N. Eigenfunctions for the case of the frequency being equal to 100 MHz are plotted in Figs. 3.8, 3.9, and 3.10 for all three boundary condition cases as indicated. As can be seen from these plots the eigenfunctions all go to zero at $\eta = 0$. This was the condition which allowed these functions to be orthogonal. Not all the components of the actual fields will necessarily go to zero at $\eta = 0$ or $\xi = 0$, but care must be exercised in the evaluation of the fields at these points. Thus, in this section, the fields derived from the potential $U(\xi,\eta)$ will be expressed analytically at these critical points. The fields derived from the potential $Q(\xi,\eta)$ will not be explicitly shown here but can be derived by a similar procedure.

Expressions for the T.E. mode fields can be obtained by substituting Eq. (3.28) into Eqs. (2.10) - (2.13). Thus

$$E_\phi = \begin{cases} \sum_n \frac{A_n}{\xi\eta} F_0\left(\lambda_n, \frac{1}{2}K\xi^2\right) F_0\left(-\lambda_n, \frac{1}{2}K\eta^2\right) & 0<\eta<\eta_o\ ,\ \xi = 0\ region\ , \\ \sum_n \frac{B_n}{\xi\eta} H_0^1\left(\lambda_n, \frac{1}{2}K\xi^2\right) F_0\left(-\lambda_n, \frac{1}{2}K\eta^2\right) & 0<\eta<\eta_o\ ,\ \xi > 0\ region\ , \end{cases} \tag{3.33}$$

$$H_\xi = \frac{-i\omega\epsilon}{\xi K\sqrt{\xi^2+\eta^2}} \times$$

$$\begin{cases} \sum_n A_n F_0\left(\lambda_n, \frac{1}{2}K\xi^2\right) F_0'\left(-\lambda_n, \frac{1}{2}K\eta^2\right) & 0<\eta<\eta_o\ ,\ \xi = 0\ region\ , \\ \sum_n B_n H_0^1\left(\lambda_n, \frac{1}{2}K\xi^2\right) F_0'\left(-\lambda_n, \frac{1}{2}K\eta^2\right) & 0<\eta<\eta_o\ ,\ \xi > 0\ region\ , \end{cases} \tag{3.34}$$

$$H_\eta = \frac{i\omega\epsilon}{\eta K\sqrt{\xi^2+\eta^2}} \times$$

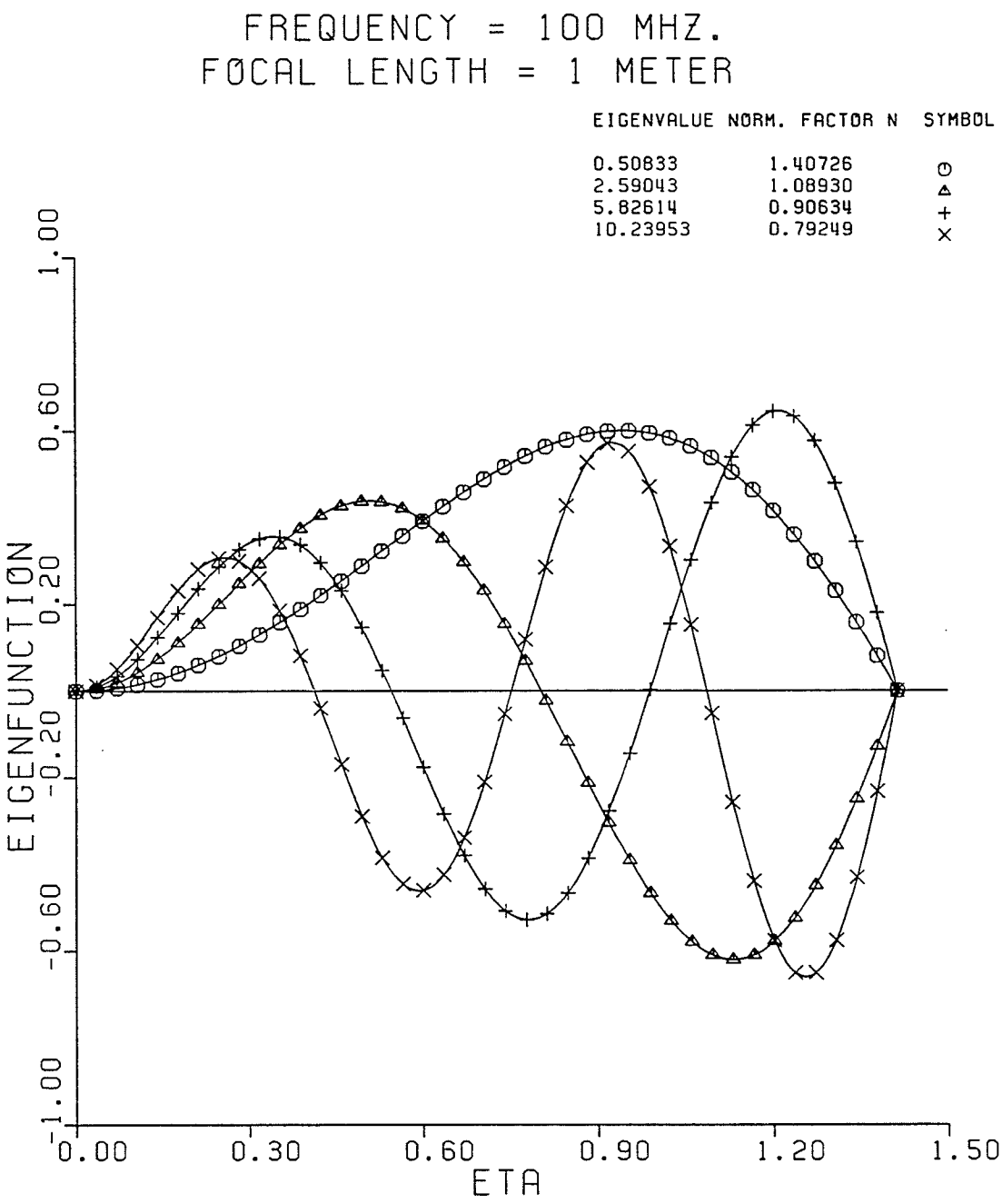

FIGURE 3.8: EIGENFUNCTIONS FOR DIRICHLET CONDITION

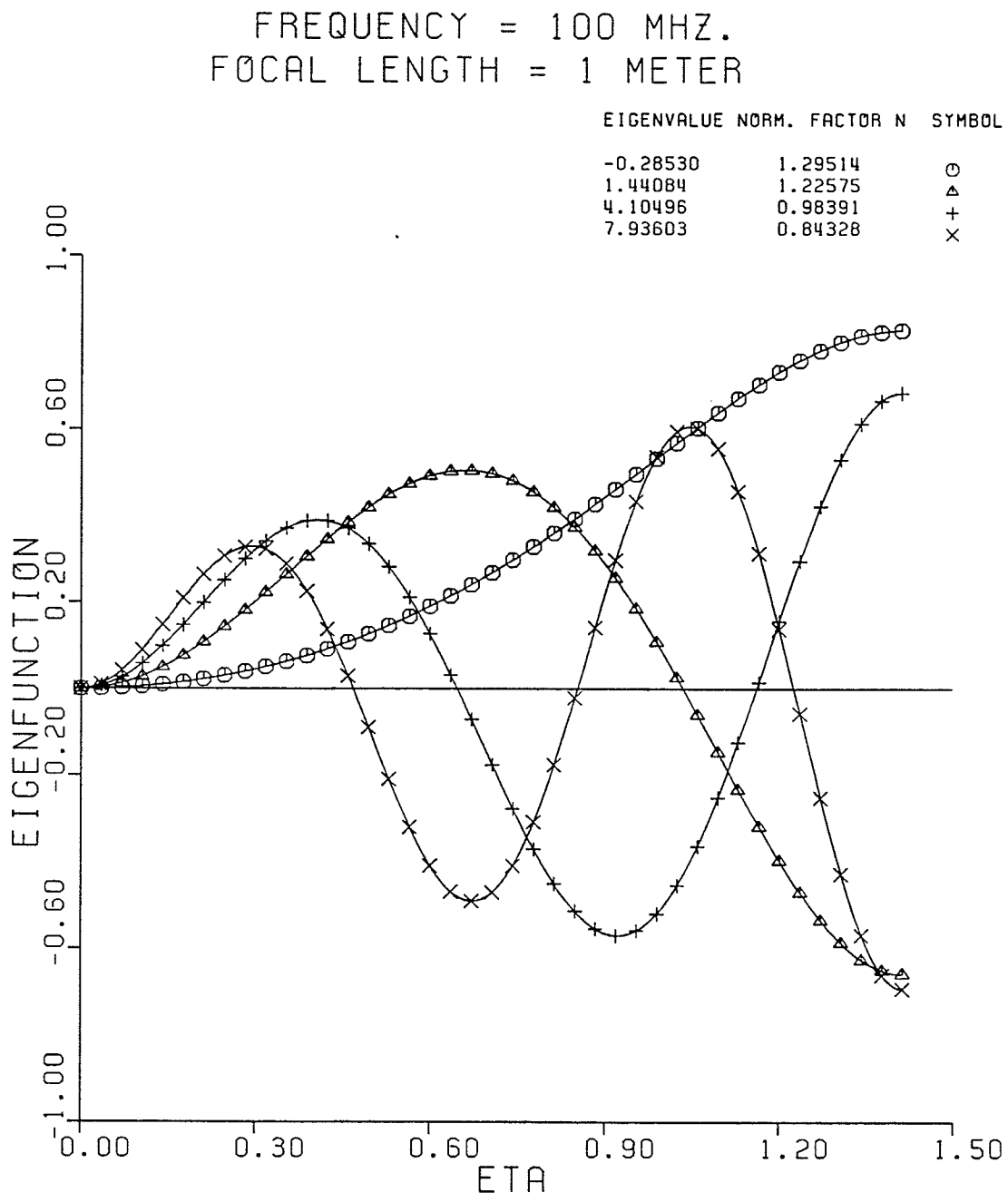

FIGURE 3.9: EIGENFUNCTIONS FOR NEUMANN CONDITION

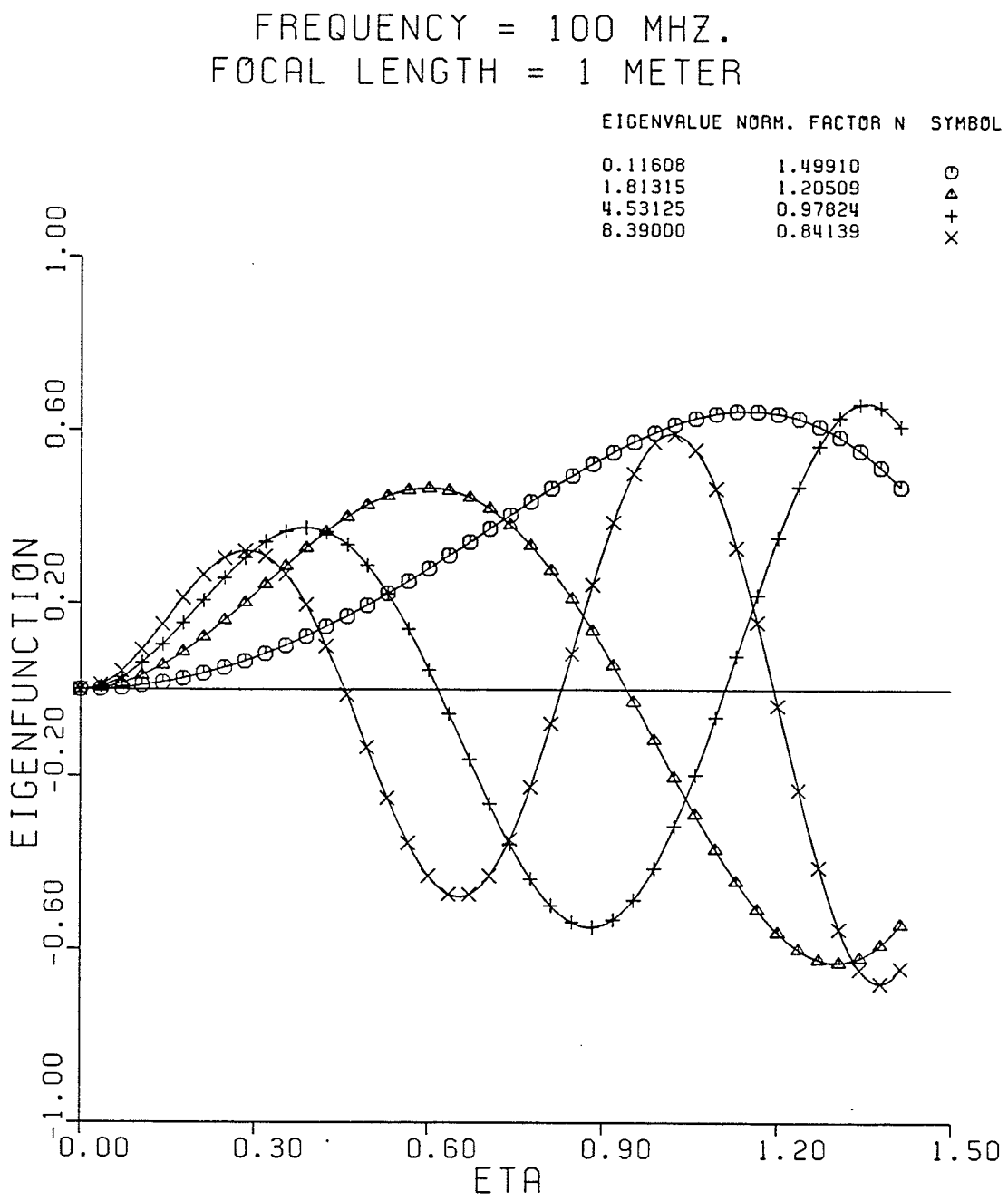

FIGURE 3.10: EIGENFUNCTIONS FOR ROBIN CONDITION

$$\begin{cases} \sum_n A_n \, F_0'\left(\lambda_n \cdot \frac{1}{2} K \xi^2\right) F_0\left(-\lambda_n \cdot \frac{1}{2} K \eta^2\right) & 0 < \eta < \eta_o \ , \ \xi = 0 \ region \ , \\ \sum_n B_n \, H_0^{1\,\prime}\left(\lambda_n \cdot \frac{1}{2} K \xi^2\right) F_0\left(-\lambda_n \cdot \frac{1}{2} K \eta^2\right) & 0 < \eta < \eta_o \ , \ \xi > 0 \ region \ . \end{cases} \tag{3.35}$$

In order to evaluate these expressions on either the $\xi = 0$ axis or the $\eta = 0$ axis, the limit will be taken and L'Hopital's rule will be used throughout. As $\eta \to 0$ the fields become

$$E_\phi = 0 \quad \eta = 0 \ , \tag{3.36}$$

$$H_\xi = \frac{-i\,\omega\,\epsilon}{K\,\xi^2} \begin{cases} \sum_n A_n \, F_0\left(\lambda_n \cdot \frac{1}{2} K \xi^2\right) C_0\left(-\lambda_n\right) & \eta = 0 \ , \ \xi = 0 \ region \ , \\ \sum_n B_n \, H_0^1\left(\lambda_n \cdot \frac{1}{2} K \xi^2\right) C_0\left(-\lambda_n\right) & \eta = 0 \ , \ \xi > 0 \ region \ , \end{cases} \tag{3.37}$$

$$H_\eta = 0 \quad \eta = 0 \ . \tag{3.38}$$

As can be seen at $\eta = 0$ only the H_ξ component survives. This is consistent with expectations since the field must be symmetric in ϕ.

As $\xi \to 0$ the fields become

$$E_\phi = 0 \quad \xi = 0 \ , \tag{3.39}$$

$$H_\xi = 0 \quad \xi = 0 \ , \tag{3.40}$$

$$H_\eta = \frac{i\,\omega\,\epsilon}{K\,\eta^2} \sum_n A_n \, C_0\left(\lambda_n\right) F_0\left(-\lambda_n \cdot \frac{1}{2} K \eta^2\right) \quad 0 < \eta < \eta_o \ , \ \xi = 0 \ . \tag{3.41}$$

This time only the η component of the magnetic field survives, as expected.

CHAPTER 4

CURRENT LOOP EXCITATION

Thus far, eigenfunctions and eigenvalues have been obtained for the representation of rotationally symmetric fields inside the paraboloid. In this chapter the eigenfunctions are used to represent the fields due to geometrically simple electric sources. Specifically, the fields due to an electric current loop centered about the axis of the paraboloid are determined. The procedure follows closely that of determining the fields inside a conical waveguide due to a similar type excitation (see Harrington [1961], Hadidi [1985]). Although only electric current sources will be considered herein, magnetic current sources can be handled in an identical manner.

4.1 Formulation of the Problem

Consider the case of an electric current sheet which is symmetric about the z axis interior to an infinite paraboloid . The current sheet may be expressed by the following equation :

$$\bar{J}\,(\,\xi\,,\,\eta\,) = J_{\phi}(\eta)\,\delta(\,\xi - \xi^{*}\,)\,\hat{a}_{\phi}\,. \tag{4.1}$$

In Eq. (4.1) $\delta(\,\xi - \xi^{*}\,)$ represents, as usual, the impulse function and $J_{\phi}(\eta)$ represents the magnitude of the current sheet. The dependence on η of the magnitude $J_{\phi}(\eta)$ is not shown explicitly since it is arbitrary. In order to simulate a current ring the η dependence will be set equal to the impulse function as well.

It is obvious that this specific excitation of Eq. (4.1) will produce fields which are independent of the coordinate ϕ. Thus the Abraham potentials are appropriate and in fact it will become apparent that only the potential U will be necessary since the fields will be transverse electric (T.E.) to the z axis.

The potential U can be represented in terms of an infinite summation of eigenfunctions as shown below in Eq. (4.2). Note that the Coulomb wave function of the third kind is used in region II (ie. in the region where $\xi > \xi^*$). The reason for this is that outward travelling waves are desired in region II and these are best represented by wave functions of the third kind.

$$U(\xi,\eta) = \begin{cases} \sum_n A_n F_0\left(\frac{C_n}{4K}, \frac{1}{2}K\xi^2\right) F_0\left(\frac{-C_n}{4K}, \frac{1}{2}K\eta^2\right) & 0<\xi<\xi^*, 0<\eta<\eta_o, \\ \sum_n B_n H_0^1\left(\frac{C_n}{4K}, \frac{1}{2}K\xi^2\right) F_0\left(\frac{-C_n}{4K}, \frac{1}{2}K\eta^2\right) & \xi>\xi^*, 0<\eta<\eta_o. \end{cases} \tag{4.2}$$

The summation over n in Eq. (4.2) represents a summation over the ordered eigenvalues where the eigenvalues $\lambda_n = C_n/4K$ are obtained from the transcendental equation produced by applying the boundary conditions on the walls of the waveguide. The following discussion will proceed independent of the boundary conditions on the walls of the waveguide. All that will be assumed is that a transcendental equation can be found and solved, producing the eigenvalues necessary in the following equations.

The field expressions can now be obtained from the potential U. Note that since the field will be T.E. to the z direction, this implies that $E_\xi = E_\eta = H_\phi = 0$. Hence,

$$E_\phi(\xi,\eta) = \frac{1}{\rho} U(\xi,\eta) \tag{4.3}$$

$$H_\xi(\xi,\eta) = \frac{-i\omega\epsilon}{\rho K^2\sqrt{\xi^2+\eta^2}} \frac{\partial U(\xi,\eta)}{\partial \eta} \tag{4.4}$$

$$H_\eta(\xi,\eta) = \frac{i\omega\epsilon}{\rho K^2\sqrt{\xi^2+\eta^2}} \frac{\partial U(\xi,\eta)}{\partial \xi} \tag{4.5}$$

The continuity of E_ϕ at $\xi = \xi^*$ must now be imposed on Eq. (4.3) and from this

$$\frac{-i\,\eta K\sqrt{\xi^{*2}+\eta^2}}{\omega\epsilon}\,J_\phi(\eta)=\sum_n B_n\left\{\frac{H_0^{1\prime}F_0-F_0'H_0^1}{F_0\left(\frac{C_n}{4K},\frac{1}{2}K\xi^{*2}\right)}\right\}\times F_0\left(\frac{-C_n}{4K},\frac{1}{2}K\eta^2\right),\quad(4.10)$$

where the argument of the wave functions in the numerator are the same as that of the denominator. Now recalling the wronskian relation for the Coulomb wave functions

$$F_0'G_0-F_0G_0'=1,$$

and recalling that

$$H_0^1=G_0+iF_0$$

it is seen that

$$H_0^{1\prime}F_0-F_0'H_0^1=\left[G_0'+iF_0'\right]F_0-F_0'\left[G_0+iF_0\right]=G_0'F_0-G_0F_0'=-1.$$

Thus Eq. (4.10) becomes

$$\frac{i\,\eta K\sqrt{\xi^{*2}+\eta^2}}{\omega\epsilon}\,J_\phi(\eta)=\sum_n\left\{\frac{B_n}{F_0\left(\frac{C_n}{4K},\frac{1}{2}K\xi^{*2}\right)}\right\}F_0\left(\frac{-C_n}{4K},\frac{1}{2}K\eta^2\right).\quad(4.11)$$

Now Eq. (4.11) can be recognized as the generalized Fourier transform of the function on the left with Fourier coefficient being enclosed in the brackets. Therefore using the orthogonality property of the regular Coulomb wave functions, which was derived in chapter 3, the coefficients B_n can be obtained. Multiplying Eq. (4.11) by $2/z\,F_0(\frac{-C_n}{4K},z)$, where $z=\frac{1}{2}K\eta^2$, and integrating over the range $0<z<z_o$, where $z_o=\frac{1}{2}K\eta_o^2$, we arrive at

condition the following is obtained :

$$A_n F_0\left(\frac{C_n}{4k}, \frac{1}{2} K \xi^{*2}\right) = B_n H_0^1\left(\frac{C_n}{4k}, \frac{1}{2} K \xi^{*2}\right) ,$$

and thus,

$$A_n = B_n \frac{H_0^1\left(\frac{C_n}{4K}, \frac{1}{2} K \xi^{*2}\right)}{F_0\left(\frac{C_n}{4K}, \frac{1}{2} K \xi^{*2}\right)} . \tag{4.6}$$

Also, the appropriate boundary condition at a current source must be applied. This can be expressed in vector form as

$$\hat{n} \times \left(\bar{H}^{(I)} - \bar{H}^{(II)}\right) = \bar{J}_s (\xi, \eta) . \tag{4.7}$$

where $\hat{n}$ is the unit normal into region (I) and $\bar{J}_s$ is the current sheet at the interface between region (I) and region (II). For the specific case under consideration here, $\hat{n} = -\hat{a}_\xi$ and $\bar{J}_s = \bar{J}$ of Eq. (4.1). Thus applying the boundary condition of Eq. (4.7) to the problem at hand at $\xi = \xi^*$ we get

$$H_\eta^{(II)} (\xi^*, \eta) - H_\eta^{(I)} (\xi^*, \eta) = J_\phi (\eta) \delta (\xi^* - \xi^*) \hat{a}_\phi = J_\phi (\eta) \hat{a}_\phi . \tag{4.8}$$

Substituting the expression of Eq. (4.5) into Eq. (4.8) one obtains

$$J_\phi (\eta) = \frac{i \omega \epsilon}{\eta K \sqrt{\xi^{*2} + \eta^2}} \times$$

$$\sum_n \left\{ B_n H_0^{1\prime}\left(\frac{C_n}{4K}, \frac{1}{2} K \xi^{*2}\right) - A_n F_0'\left(\frac{C_n}{4K}, \frac{1}{2} K \xi^{*2}\right) \right\} F_0\left(\frac{C_n}{4K}, \frac{1}{2} K \eta^2\right), \tag{4.9}$$

where the prime represents differentiation with respect to the argument $z = \frac{1}{2} K \xi^2$. Applying Eq. (4.6) to the result of Eq. (4.9) and performing some algebraic manipulations we arrive at

$$B_n = \frac{i\,K}{\omega \epsilon N_n^2} F_0\left(\frac{C_n}{4K}, \frac{1}{2} K \xi^{*2}\right) \int_0^{z_o} \eta \sqrt{\xi^{*2} + \eta^2} \left(\frac{2}{z}\right) J_\phi(\eta) F_0\left(\frac{-C_n}{4K}, z\right) dz \,,$$

or

$$B_n = \frac{i\,4K}{\omega \epsilon N_n^2} F_0\left(\frac{C_n}{4K}, \frac{1}{2} K \xi^{*2}\right) \int_0^{\eta_o} \sqrt{\xi^{*2} + \eta^2} J_\phi(\eta) F_0\left(\frac{-C_n}{4K}, \frac{1}{2} K \eta^2\right) d\eta \,, \qquad (4.12)$$

where N_n represents the normalization constant for each eigenvalue.

If it is assumed that the current sheet becomes a current ring then $J_\phi(\eta)$ can be expressed as

$$J_\phi(\eta) = J_{loop}\, \delta(\eta - \eta^*) \quad with \quad \eta^* \leq \eta_o \,, \qquad (4.13)$$

where J_{loop} represents the magnitude of the current flowing in the loop. Substitution of this into Eq. (4.12) yields

$$B_n = \frac{i\,4K\,J_{loop}\sqrt{\xi^{*2} + \eta^{*2}}}{\omega \epsilon N_n^2} F_0\left(\frac{-C_n}{4K}, \frac{1}{2} K \eta^{*2}\right) F_0\left(\frac{C_n}{4K}, \frac{1}{2} K \xi^{*2}\right) , \qquad (4.14)$$

and from Eq. (4.6)

$$A_n = \frac{i\,4K\,J_{loop}\sqrt{\xi^{*2} + \eta^{*2}}}{\omega \epsilon N_n^2} F_0\left(\frac{-C_n}{4K}, \frac{1}{2} K \eta^{*2}\right) H_0^1\left(\frac{C_n}{4K}, \frac{1}{2} K \xi^{*2}\right) . \qquad (4.15)$$

As can be seen from Eq. (4.14) and Eq. (4.15) the series coefficients A_n and B_n are only functions of the eigenvalue, as the notation used (n subscript) would imply. If J_{loop} is set to

$$J_{loop} = \frac{\omega \epsilon}{4K\sqrt{\xi^{*2} + \eta^{*2}}} \qquad (4.16)$$

then the equations for the coefficients simplify to

$$B_n = \frac{i}{N_n^2} F_0\left(\frac{-C_n}{4K}, \frac{1}{2}K\eta^{*2}\right) F_0\left(\frac{C_n}{4K}, \frac{1}{2}K\xi^{*2}\right), \tag{4.17}$$

and

$$A_n = \frac{i}{N_n^2} F_0\left(\frac{-C_n}{4K}, \frac{1}{2}K\eta^{*2}\right) H_0^1\left(\frac{C_n}{4K}, \frac{1}{2}K\xi^{*2}\right). \tag{4.18}$$

These equations were used to calculate the first few coefficients for a paraboloid with focal length equal to 1 meter and source frequencies of 100 MHz., 250 MHz., and 500 MHz. These frequencies were used because the eigenvalues were calculated for these frequencies in the previous chapter. Calculations were made for a current ring of radius ½ meter located in the plane of the focal point. This current ring can be represented by letting $\xi^* = \frac{1}{\sqrt{2}}$ and $\eta^* = \frac{1}{\sqrt{2}}$. Note that both these coordinates have the same value since the ring is located in the focal plane. As a check, the radius of the ring r is given by

$$r = \xi^* \eta^* = \frac{1}{2} meter, \tag{4.19}$$

which is what we required. The coefficients for the Dirichlet boundary condition are shown in Table 4.1 for all three frequencies. The Neumann and the Robin boundary condition cases are also shown in Tables 4.2 and 4.3, respectively.

As can be seen from viewing the tables, the coefficients become smaller and smaller as the mode number n increases. This is what would be expected to happen since similar results appear in conical waveguides and other waveguides. Thus only the first few modes actually propagate down the waveguide with the higher order modes being highly attenuated.

TABLE 4.1

Eigenvalues and Series Coefficients for the Dirichlet Case

Focal Length = 1 meter

100 MHz		250 MHz		500 MHz	
λ_n	B_n / i	λ_n	B_n / i	λ_n	B_n / i
0.5083	0.8315×10^{-1}	-0.7868	0.9134×10^{-1}	-2.8482	0.3022×10^{-1}
2.5904	0.3975×10^{-3}	0.3574	0.2402	-1.3326	-0.1819
5.8261	-0.1634×10^{-6}	1.6424	-0.2067×10^{-1}	-0.2952	-0.3992×10^{-1}
10.2400	-0.3671×10^{-12}	3.3919	-0.7448×10^{-3}	0.5911	-0.2203
		5.6191	0.3648×10^{-5}	1.6480	-0.5856×10^{-1}
		8.3209	0.3667×10^{-8}	2.9597	0.1915×10^{-1}
				4.5213	-0.1423×10^{-4}
				6.3269	-0.2087×10^{-4}
				8.3735	0.5161×10^{-7}

TABLE 4.2

Eigenvalues and Series Coefficients for the Neumann Case

Focal Length = 1 meter

100 MHz		250 MHz		500 MHz	
λ_n	B_n / i	λ_n	B_n / i	λ_n	B_n / i
-0.2853	0.1300	-1.7051	$-.3375\times10^{-1}$	-4.1067	0.1927×10^{-2}
1.4408	0.1313×10^{-1}	-0.1828	0.3030	-2.0163	0.1485×10^{-1}
4.1050	$-.6222\times10^{-5}$	0.9510	0.3765×10^{-1}	-0.7743	-.2924
7.9360	-0.5142×10^{-9}	2.4663	-0.7351×10^{-2}	0.1426	0.4041×10^{-1}
		4.4589	-0.1253×10^{-5}	1.0895	-0.2495
		6.9264	0.1963×10^{-6}	2.2746	0.2932×10^{-1}
		9.8667	-0.1071×10^{-10}	3.7134	0.3661×10^{-2}
				5.3987	-0.1221×10^{-3}
				7.3261	-0.1208×10^{-5}
				9.4931	0.1260×10^{-7}

TABLE 4.3

Eigenvalues and Series Coefficients for the Robin Case

Focal Length = 1 meter

100 MHz		250 MHz		500 MHz	
λ_n	B_n / i	λ_n	B_n / i	λ_n	B_n / i
0.1161	0.1088	-1.1043	0.1087×10^{-1}	-3.2193	0.1642×10^{-1}
1.8132	0.4580×10^{-2}	0.0852	0.3032	-1.6168	-0.7445×10^{-1}
4.5313	-0.2984×10^{-5}	1.2410	-0.6194×10^{-2}	-0.5186	-0.1847
8.3900	-0.1319×10^{-9}	2.8113	-0.3394×10^{-2}	0.3580	-0.7900×10^{-1}
		4.8424	0.8564×10^{-5}	1.3408	-0.1604
		7.3367	0.6537×10^{-7}	2.5666	0.2932×10^{-1}
		10.2960	-0.1019×10^{-10}	4.0379	0.1215×10^{-2}
				5.7492	-0.6892×10^{-4}
				7.6977	-0.2510×10^{-6}
				9.8820	0.5416×10^{-8}

CHAPTER 5

THE FINITE PARABOLOID

Up to now the fields inside an infinite paraboloid have been determined. The logical step now is to consider the finite paraboloid and to determine the fields exterior to it. Obviously this is the much more practical situation, since this problem could be used to represent the fields of a paraboloidal reflector. In this chapter the paraboloidal reflector is treated as an aperture antenna and the *field equivalence principle* or *Huygens' Principle* is used to determine the far field from the antenna. The far field is represented in spherical coordinates $(r, \theta, \phi,)$ and is plotted as a function of θ at the end of this chapter. Of course, the assumption of symmetry of the fields with respect to ϕ is still made so that the field expressions of the previous chapters can be used. Thus the far field patterns will also be symmetric in ϕ.

5.1 Field Equivalence Principle: Huygens' Principle

The field equivalence principle is a stricter form of Huygens' principle which allows one to replace actual sources with equivalent sources. Huygens' principle can be summarized by the following excerpt from Kraus and Carver [1973]

> *each point on a primary wavefront can be considered to be a new source of a secondary spherical wave and that a secondary wavefront can be constructed as the envelope of the secondary spherical waves.*

The equivalence principle combines this with the *Uniqueness theorem* which can be summarized by the following excerpt from Harrington [1961]:

> *A field in a lossy region is uniquely specified by the sources within the region plus the tangential components of the electric field over the boundary, or the tangential components of the magnetic field over the boundary, or the former*

over part of the boundary and the latter over the rest of the boundary.

The problem of the finite paraboloid with current loop sources about the axis of symmetry can be transformed into an equivalent problem by considering the closed surface S shown in Fig. 5.1a. This surface S is made up of the finite paraboloid itself plus the paraboloidal aperture surface described by $\xi = \xi_o$ for $0 < \eta < \eta_o$. The outward normal on the aperture surface is given by $\hat{n} = \hat{a}_\xi$. The fields outside the surface S are denoted by $\bar{E}_1$ and $\bar{H}_1$ while the fields inside will be denoted by $\bar{E}$ and $\bar{H}$. The equivalent problem of Fig. 5.1a is shown in Fig. 5.1b. The original current loop source which was interior to the closed surface S was removed with equivalent sources $\bar{J}_s(\xi_o, \eta)$ and $\bar{M}_s(\xi_o, \eta)$ placed on the surface $\xi = \xi_o$. These equivalent sources are given by

$$\bar{J}_s = \hat{n} \times \left[\bar{H}_1 - \bar{H}\right] , \tag{5.1}$$

and

$$\bar{M}_s = -\hat{n} \times \left[\bar{E}_1 - \bar{E}\right] . \tag{5.2}$$

The current on the outside walls of the finite paraboloid is assumed to be equal to zero.

Now, by the equivalence principle, it is assumed that the equivalent sources on the surface $\xi = \xi_o$ produce the original field-$(\bar{E}_1, \bar{H}_1)$ only outside the surface S. The fields produced inside S by the equivalent sources will not in general be the same as in the original problem and in fact they can be set equal to any convenient value. A form of the equivalence principle, known as *Love's Equivalence Principle* (see Love [1901]) is now used, which sets the field inside the surface S equal to zero. This reduces Eq. (5.1) and Eq. (5.2) to

$$\bar{J}_s = \hat{n} \times \bar{H}_1 = \hat{a}_\xi \times \bar{H}_1 , \tag{5.3}$$

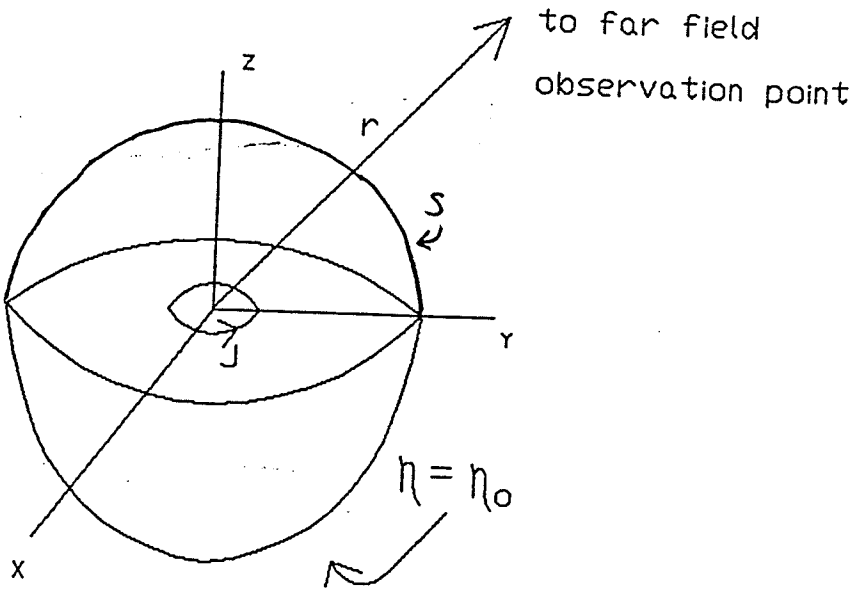

FIG. 5.1A: CURRENT LOOP INSIDE PARABOLOID

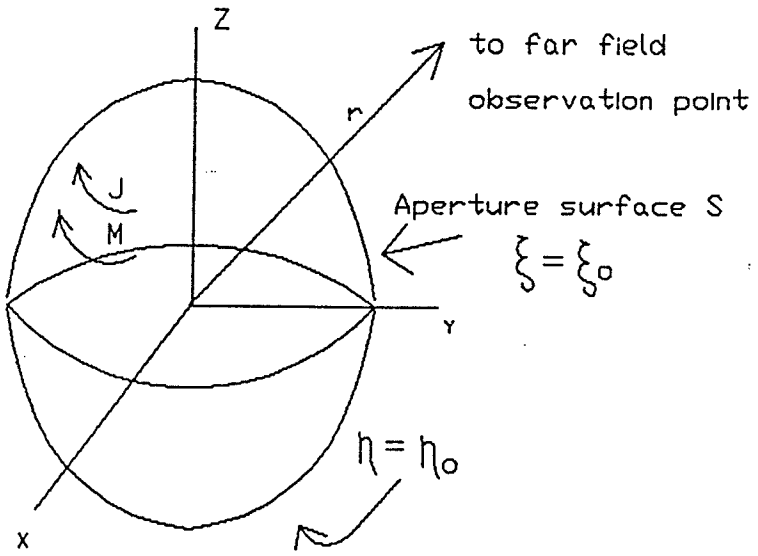

FIG. 5.1B: EQUIVALENT PROBLEM USING EQUIVALENT CURRENT SOURCES

and

$$\bar{M}_s = -\hat{n} \times \bar{E}_1 = -\hat{a}_\xi \times \bar{E}_1 \ . \tag{5.4}$$

For $\bar{E}_1$ and $\bar{H}_1$ at the surface $\xi = \xi_o$ we use the field which would have existed if the paraboloid was infinite. This is the standard procedure in the analysis of the conical horn and it will be used here because of the close resemblance between that problem and the present problem. Thus the fields over the aperture, for a current loop described by Eq. (4.16), are given by Eq. (3.33) - Eq. (3.35) at $\xi = \xi_o$ with the B_n's given by Eq. (4.17). The B_n's were calculated and tabulated in the last chapter. Thus for the problem of the current loop of chapter 4 the field will be T.E. to the z-axis and therefore Eq. (5.3) and Eq. (5.4) become

$$\bar{J}_s = H_\eta(\xi_o, \eta)\hat{a}_\phi = J_\phi(\xi_o, \eta)\hat{a}_\phi \ , \quad 0 < \eta < \eta_o \ , \tag{5.5}$$

and

$$\bar{M}_s = E_\phi(\xi_o, \eta)\hat{a}_\eta = M_\eta(\xi_o, \eta)\hat{a}_\eta \ , \quad 0 < \eta < \eta_o \ . \tag{5.6}$$

The far field can now be obtained from the equivalent sources by using the auxiliary potentials $\bar{A}$ and $\bar{F}$ where in general

$$\bar{A} = \frac{\mu}{4\pi} \int\int_V \int \bar{J} \frac{e^{-ikR}}{R} dv' \ , \tag{5.7}$$

and

$$\bar{F} = \frac{\epsilon}{4\pi} \int\int_V \int \bar{M} \frac{e^{-ikR}}{R} dv' \ . \tag{5.8}$$

The integration volume V is the volume containing the sources and the distance R is the distance from the source point to the observation point.

If we define, as usual, $\bar{r}$ as the distance from the origin to the observation point and $\bar{r}'$ as the distance from the origin to the source point then we have

$$R = \left| \bar{r} - \bar{r}' \right| . \tag{5.9}$$

For far field calculations we make the usual approximation (see Balanis [1982])

$$R \approx r - r' \cos\psi \quad , \text{for } \textit{phase term} , \tag{5.10}$$

and

$$R \approx r \quad , \text{for } \textit{amplitude term}. \tag{5.11}$$

where ψ is the angle between the vectors $\bar{r}$ and $\bar{r}'$. If these approximations are substituted into Eq. (5.7) and Eq. (5.8) and the equivalent surface current expressions are used then the far field auxiliary potentials can be expressed as

$$\bar{A} = \frac{\mu}{4\pi} \int_S \int \bar{J}_s \frac{e^{-ikR}}{R} ds' \approx \frac{\mu e^{-ikr}}{4\pi r} \bar{N}_A , \tag{5.12}$$

where

$$\bar{N}_A = \int_S \int \bar{J}_s e^{ikr' \cos\psi} ds' , \tag{5.13}$$

and

$$\bar{F} = \frac{\epsilon}{4\pi} \int_S \int \bar{M}_s \frac{e^{-ikR}}{R} ds' \approx \frac{\epsilon e^{-ikr}}{4\pi r} \bar{L}_F , \tag{5.14}$$

where

$$\bar{L}_F = \int_S \int \bar{M}_s e^{ikr' \cos\psi} ds' . \tag{5.15}$$

The vectors $\bar{N}_A$ and $\bar{L}_F$ are sometimes called the radiation vectors.

It should be noted at this point that the relations given by Eq. (5.7) and Eq. (5.8) are only valid for the rectangular components of the auxiliary potentials. Thus the required equivalent sources for use in these equations and equations derived from these must be expressed in terms of the rectangular components such as

$$\bar{J} = J_x \hat{a}_x + J_y \hat{a}_y + J_z \hat{a}_z \quad . \tag{5.16}$$

Since the fields we have determined in previous chapters are expressed in terms of rotation-paraboloidal components, such as

$$\bar{J} = J_\xi \hat{a}_\xi + J_\eta \hat{a}_\eta + J_\phi \hat{a}_\phi \quad . \tag{5.17}$$

it will be useful to write the rectangular current components for the above equations in terms of rotation-paraboloidal coordinates. To accomplish this we turn to the *law of transformation of vectors* (see Morse and Feshbach [1953]). This law states that if we transform the components of a vector $\bar{F}$ from one curvilinear coordinate system (ξ_1, ξ_2, ξ_3) with scale factors (h_1, h_2, h_3) to another coordinate system (ξ'_1, ξ'_2, ξ'_3) with scale factors (h'_1, h'_2, h'_3), then the components in the new system must be related to the components in the old system by the relations

$$F'_n = \sum_m \gamma_{nm} F_m \quad , \tag{5.18}$$

where

$$\gamma_{nm} = \left(\frac{h_m}{h'_n}\right)\left(\frac{\partial \xi_m}{\partial \xi'_n}\right) = \left(\frac{h'_n}{h_m}\right)\left(\frac{\partial \xi'_n}{\partial \xi_m}\right) \quad . \tag{5.19}$$

The rectangular coordinates are related to the rotation-paraboloidal coordinates by the relations

$$\begin{cases} x = \xi\,\eta\cos\phi \ , \\ y = \xi\,\eta\sin\phi \ , \\ z = \dfrac{1}{2}\left(\xi^2-\eta^2\right) \ , \end{cases} \tag{5.20}$$

with scale factors given by

$$\begin{cases} h_1 = \sqrt{\xi^2+\eta^2} \ , \\ h_2 = \sqrt{\xi^2+\eta^2} \ , \\ h_3 = \xi\,\eta \ . \end{cases} \tag{5.21}$$

Thus with the help of Eq. (5.18), the transformation from rotation-paraboloidal components to rectangular components can be written as

$$J_x = \frac{\eta'\cos\phi'}{\sqrt{\xi'^2+\eta'^2}}J_\xi + \frac{\xi'\cos\phi'}{\sqrt{\xi'^2+\eta'^2}}J_\eta - \sin\phi' J_\phi \ , \tag{5.22a}$$

$$J_y = \frac{\eta'\sin\phi'}{\sqrt{\xi'^2+\eta'^2}}J_\xi + \frac{\xi'\sin\phi'}{\sqrt{\xi'^2+\eta'^2}}J_\eta + \cos\phi' J_\phi \ , \tag{5.22b}$$

$$J_z = \frac{\xi'}{\sqrt{\xi'^2+\eta'^2}}J_\xi - \frac{\eta'}{\sqrt{\xi'^2+\eta'^2}}J_\eta \ . \tag{5.22c}$$

Similar results are also obtained for the components of the magnetic current density required in Eq. (5.15).

Since the radiated fields are usually determined in spherical components, the rectangular unit vectors of Eq. (5.16) can be transformed into spherical unit vectors using the transformation from rectangular components to spherical components given by

$$\begin{cases} \hat{a}_x = \hat{a}_r\sin\theta\cos\phi + \hat{a}_\theta\cos\theta\cos\phi - \hat{a}_\phi\sin\phi \ , \\ \hat{a}_y = \hat{a}_r\sin\theta\sin\phi + \hat{a}_\theta\cos\theta\sin\phi + \hat{a}_\phi\cos\phi \ , \\ \hat{a}_z = \hat{a}_r\cos\theta - \hat{a}_\theta\sin\theta \ . \end{cases} \tag{5.23}$$

The variables in these expressions are not primed as they were in Eq. (5.22) since

there they represented coordinates at the source points and in this transformation they represent coordinates at the observation points.

Theoretically, the auxiliary potentials could now be calculated by substituting Eq. (5.23) and Eq. (5.22) into Eqs. (5.12) and (5.14). Our problem will be greatly simplified because not all the components of the current densities exist. It will be more convenient to hold off the calculations until expressions for the actual far fields are obtained.

5.2 The Far Field Expressions

Once the auxiliary potentials have been found, the fields can be obtained from the relations

$$\bar{E} = -i\,\omega\bar{A} - i\,\frac{1}{\omega\,\mu\,\epsilon}\nabla\,(\nabla\cdot\bar{A}) - \frac{1}{\epsilon}\nabla\times\bar{F}\ , \tag{5.24}$$

and

$$\bar{H} = \frac{1}{\mu}\nabla\times\bar{A} - i\,\omega\bar{F} - i\,\frac{1}{\omega\,\mu\,\epsilon}\nabla\,(\nabla\cdot\bar{F})\ . \tag{5.25}$$

It can be shown (see Balanis [1982], p.455) that the far field can be approximated by the set of relations

$$\begin{cases} E_r(\theta,\phi) \approx 0\ , \\ E_\theta(\theta,\phi) \approx \dfrac{-iK}{4\pi r}\,e^{-iKr}\left(L_{F\phi} + \sqrt{\dfrac{\mu}{\epsilon}}\,N_{A\theta}\right)\ , \\ E_\phi(\theta,\phi) \approx \dfrac{iK}{4\pi r}\,e^{-iKr}\left(L_{F\theta} - \sqrt{\dfrac{\mu}{\epsilon}}\,N_{A\phi}\right)\ , \end{cases} \tag{5.26}$$

and

$$\begin{cases} H_r(\theta,\phi) \approx 0 \ , \\ H_\theta(\theta,\phi) \approx \dfrac{iK}{4\pi r} e^{-iKr}\left[N_{A\phi} - \sqrt{\dfrac{\epsilon}{\mu}} L_{F\theta}\right] \ , \\ H_\phi(\theta,\phi) \approx \dfrac{-iK}{4\pi r} e^{-iKr}\left[N_{A\theta} + \sqrt{\dfrac{\epsilon}{\mu}} L_{F\phi}\right] \ , \end{cases} \tag{5.27}$$

where the $N_{A\theta}$, $N_{A\phi}$, $L_{F\theta}$, and $L_{F\phi}$ are obtained from Eq. (5.13) and Eq. (5.15) and are functions of θ and ϕ. Thus to obtain the far field , all that is required is that we solve Eq. (5.26) and Eq. (5.27). This, in turn, entails solving for $N_{A\theta}$, $N_{A\phi}$, $L_{F\theta}$, and $L_{F\phi}$. After all the coordinate transformations have been applied to the electric and magnetic current densities of Eq. (5.5) and Eq. (5.6) and after extensive simplifications, the required radiation vectors can be expressed as

$$N_{A\theta} = \xi_o \cos\theta \int_0^{2\pi\eta_o}\int_0 \sin\left(\phi - \phi'\right) J_\phi(\xi_o,\eta') e^{iK\Theta} \eta' \sqrt{\xi_o^2 + \eta'^2}\, d\eta' d\phi' \ , \tag{5.28}$$

$$N_{A\phi} = \xi_o \int_0^{2\pi\eta_o}\int_0 \cos\left(\phi - \phi'\right) J_\phi(\xi_o,\eta') e^{iK\Theta} \eta' \sqrt{\xi_o^2 + \eta'^2}\, d\eta' d\phi' \ , \tag{5.29}$$

$$L_{F\theta} = \xi_o \int_0^{2\pi\eta_o}\int_0 \left[\xi_o \cos\theta \cos\left(\phi - \phi'\right) + \eta' \sin\theta\right] M_\eta(\xi_o,\eta') e^{iK\Theta} \eta' d\eta' d\phi' \ , \tag{5.30}$$

$$L_{F\phi} = \xi_o^2 \int_0^{2\pi\eta_o}\int_0 \sin\left(\phi' - \phi\right) M_\eta(\xi_o,\eta') e^{iK\Theta} \eta' d\eta' d\phi' \ , \tag{5.31}$$

where

$$\Theta = \left[\xi_o \eta' \sin\theta \cos\left(\phi - \phi'\right) + \frac{1}{2}\left(\xi_o^2 - \eta'^2\right)\cos\theta\right] \ . \tag{5.32}$$

From Eqs. (5.5) and (5.6) and from chapter 4, the equivalent current densities can be expressed as

$$J_\phi(\xi_o,\eta') = H_\eta(\xi_o,\eta')$$

$$= \frac{i\omega\epsilon}{\eta' K\sqrt{\xi_o^2+\eta'^2}} \sum_n B_n H_0^{1'}(\lambda_n, \frac{1}{2}K\xi_o^2) F_0(-\lambda_n, \frac{1}{2}K\eta'^2), \qquad (5.33)$$

and

$$M_\eta(\xi_o,\eta') = E_\phi(\xi_o,\eta')$$

$$= \frac{1}{\xi_o\eta'} \sum_n B_n H_0^1(\lambda_n, \frac{1}{2}K\xi_o^2) F_0(-\lambda_n, \frac{1}{2}K\eta'^2). \qquad (5.34)$$

These expressions can now be substituted into Eqs. (5.28) - (5.32). Since the summation is over n, the summation sign can be brought outside the integral. Thus we can express the radiation vector components, for each mode n, as

$$N_{A\theta_n} = \frac{i\omega\epsilon}{K} B_n \xi_o \cos\theta H_0^{1'}(\lambda_n, \frac{1}{2}K\xi_o^2) \times$$

$$\int_0^{2\pi}\int_0^{\eta_o} \sin(\phi-\phi') F_0(-\lambda_n, \frac{1}{2}K\eta'^2) e^{iK\Theta} d\eta' d\phi', \qquad (5.35)$$

$$N_{A\phi_n} = \frac{i\omega\epsilon}{K} B_n \xi_o H_0^{1'}(\lambda_n, \frac{1}{2}K\xi_o^2) \times$$

$$\int_0^{2\pi}\int_0^{\eta_o} \cos(\phi-\phi') F_0(-\lambda_n, \frac{1}{2}K\eta'^2) e^{iK\Theta} d\eta' d\phi', \qquad (5.36)$$

$$L_{F\theta_n} = B_n H_0^1(\lambda_n, \frac{1}{2}K\xi_o^2) \times$$

$$\int_0^{2\pi}\int_0^{\eta_o} \left[\xi_o \cos\theta\cos(\phi-\phi') + \eta' \sin\theta\right] F_0(-\lambda_n, \frac{1}{2}K\eta'^2) e^{iK\Theta} d\eta' d\phi', \qquad (5.37)$$

and

$$L_{F\phi_n} = B_n \xi_o H_0^1(\lambda_n, \frac{1}{2}K\xi_o^2) \times$$

$$\int_0^{2\pi\eta_o}\int_0^{} \sin(\phi' - \phi) F_0(-\lambda_n, \frac{1}{2}K\eta'^2) e^{iK\Theta} d\eta' d\phi' . \qquad (5.38)$$

The radiation vectors can be obtained from the above expressions by applying a summation over n. This should turn out to be neccessary for the first few terms only because the series coefficients B_n, shown in the tables of chapter 4, converge rapidly. In principle this is fine, but when one actually tries these computations problems arise. The problem with the determination of these radiation vector components is in the calculation of the Coulomb wave function of the third kind which is present in all four expressions of Eq. (5.35) - (5.38). Calculation of these functions entails calculation of the logarithmic Coulomb wave functions which are in general very difficult to compute. The problem arises because of the need for values of the logarithmic function for negative parameter. That is, when the eigenvalue λ_n is negative, which is the case for the first few modes, the parameter for which the logarithmic wave function must be calculated is also negative as can be seen in the expressions. Now this is not a problem for the regular wave functions because we have a series representation which converges fairly well, but for the logarithmic functions the series representation does not yield to simple computations. The alternative would naturally be to integrate the equation, with the negative parameter, using a method such as the Runge-Kutta method, but this is useless without some initial values for the function and its derivative. The function values at the turning points, which were used in chapter 3, are of no use because these are defined for a positive parameter only. The function value at $z = 0$ is defined by Eq. (3.21) but its derivative, which would also be required in the Runge-Kutta technique, is undefined as can be seen from Eq. (3.22). There are no other published results which would give us starting values when the parameter is negative. This is primarily due to the fact that in the field of nuclear physics, where these functions are normally

encountered, a negative parameter has no physical significance. Thus the computation of the exact radiated field would have to be left until a useful computation technique is found for calculating the logarithmic Coulomb wave function when the parameter is negative. Results can be obtained for the 100 MHz Dirichlet and Robin case since all the eigenvalues are positive for those cases.

For now the way we will get around this barrier is by calculating the radiation field for only one mode in the series expansion except for the 100 MHz Dirichlet and Robin cases as mentioned above. It will turn out that the far field plots for the first mode will not enthral us with a lot of information about the total far field due to a current ring but they are presented just the same for completeness. This will allow us to set the wave function of the third kind to 1 in the radiation vector components of Eq. (5.35) - (5.38).

Once the far field has been calculated from Eqs. (5.26) and (5.27) it is a simple matter to calculate the radiation intensity $U(\theta,\phi)$. The radiation intensity can be formulated from the far-zone electric and magnetic field components as

$$U(\theta,\phi) = \frac{1}{2}\,Real\left[\left(\hat{a}_\theta E_\theta + \hat{a}_\phi E_\phi\right) \times \left(\hat{a}_\theta H_\theta + \hat{a}_\phi H_\phi\right)^*\right]$$

$$= \frac{1}{2}\sqrt{\frac{\epsilon}{\mu}}\left(\left|E_\theta\right|^2 + \left|E_\phi\right|^2\right), \tag{5.39}$$

where the asterisk superscript denotes the complex conjugate of the expression in the brackets.

Substituting Eq. (5.26) into Eq. (5.39) and normalizing the result, we obtain the relative radiation intensity $F(\theta,\phi)$ as

$$F(\theta,\phi) = \frac{U(\theta,\phi)}{N_u} = \left|L_{F\phi} + \sqrt{\frac{\mu}{\epsilon}}N_{A\theta}\right|^2 + \left|L_{F\theta} - \sqrt{\frac{\mu}{\epsilon}}N_{A\phi}\right|^2, \tag{5.40}$$

where N_u is the required normalization constant.

5.3 Numerical Results

The integrals of Eqs. (5.36) - (5.38) are not easy to perform analytically. Thus they were performed numerically using a 20×20 point Gauss-Legendre Quadrature algorithm. The problem which was solved was for the dominant mode of a current loop with a ½ meter radius located in the plane of the focal point of the paraboloid. Calculations were performed for all three types of boundary conditions and for all three previous frequencies of 100 MHz, 250 MHz. and 500 MHz. The exact result for the 100 MHz Dirichlet case and the 100 MHz Robin case were obtained and the relative radiation intensities are shown in Fig. 5.2. The size of the paraboloid was chosen to be of 1 meter focal length as in previouse calculations. It was also assumed that the walls of the paraboloid extended up to, but not beyond, the focal plane. Thus the aperture surface is described by the coordinate surface

$$\xi = \xi_o = \eta_o \quad , \quad 0 < \eta < \eta_o \quad , \tag{5.41}$$

where η_o corresponds to a focal length of 1 meter and is related to the focal length f by

$$\eta_o = \sqrt{2f} \quad . \tag{5.42}$$

The relative radiation intensity $F(\theta, \phi)$ was plotted as a function of θ for theta ranging from 0 to 90 degrees at three degree intervals. Of course, because the fields are symmetric in ϕ, the relative radiation intensity function will be independent of ϕ and thus to simplify the equations ϕ was set equal to zero degrees. The three plots corresponding to the three boundary conditions for the dominant mode only are shown in Figs. 5.3 - 5.5.

As can be seen from Fig. 5.2, the impedance boundary condition has an effect on the far field radiation pattern. This is what we would expect since the field distribution inside the paraboloid is changed. The radiation pattern due to the impedance boundary condition case seems to give a more omnidirectional pattern than the

perfectly conducting case. Thus it seems that the Coulomb wave functions give accurate results for the far field of a current loop inside the paraboloid.

The far field plots due to the first single mode do not seem to tell us too much about the total field. If single modes could be excited inside the paraboloid then these plots could be useful. Efficient calculating methods are desperately required in order that the total field such as the one plotted in Fig. 5.2 may be obtained for the general case and thus firmly establish the method.

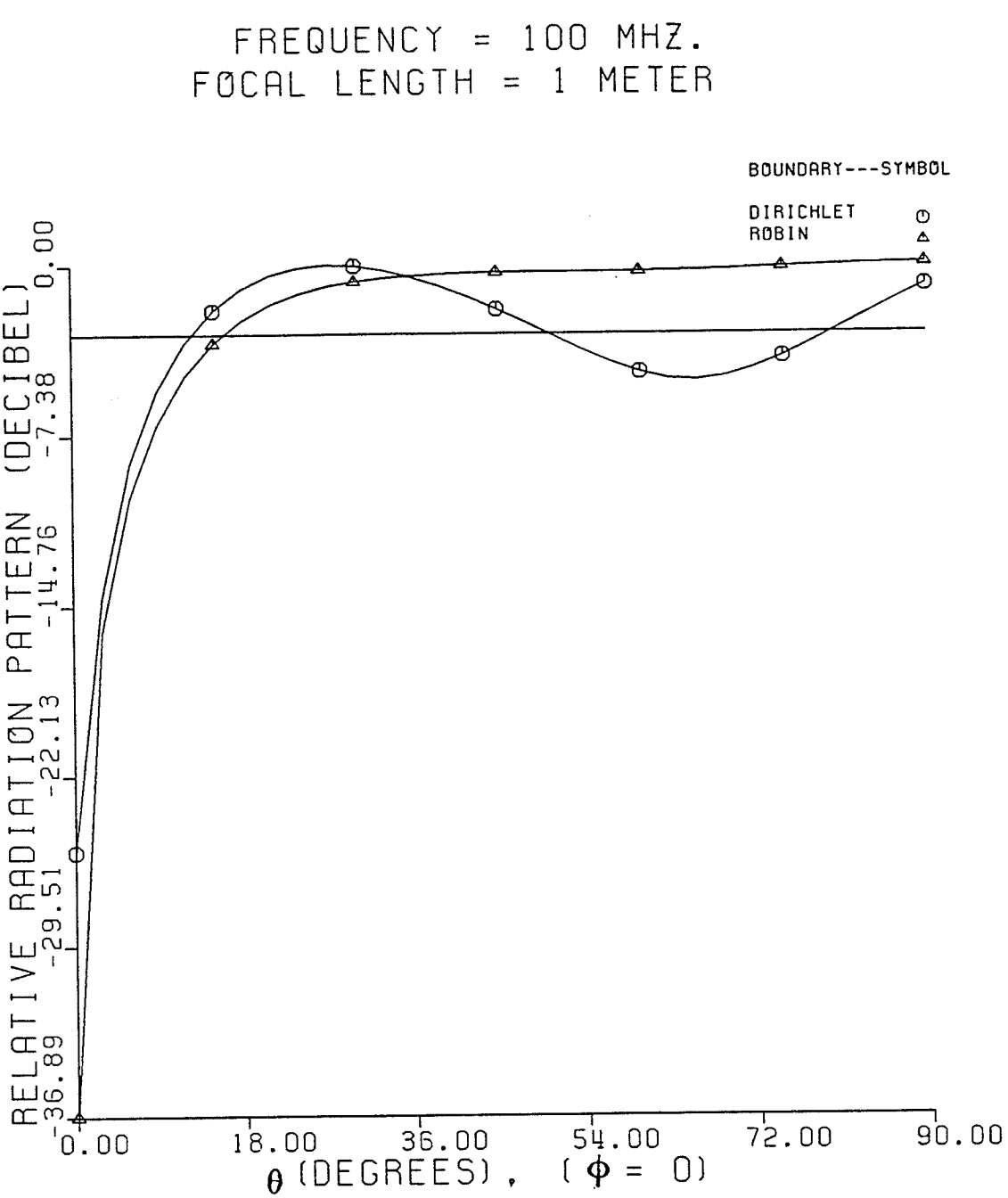

FIG. 5.2: FAR FIELD

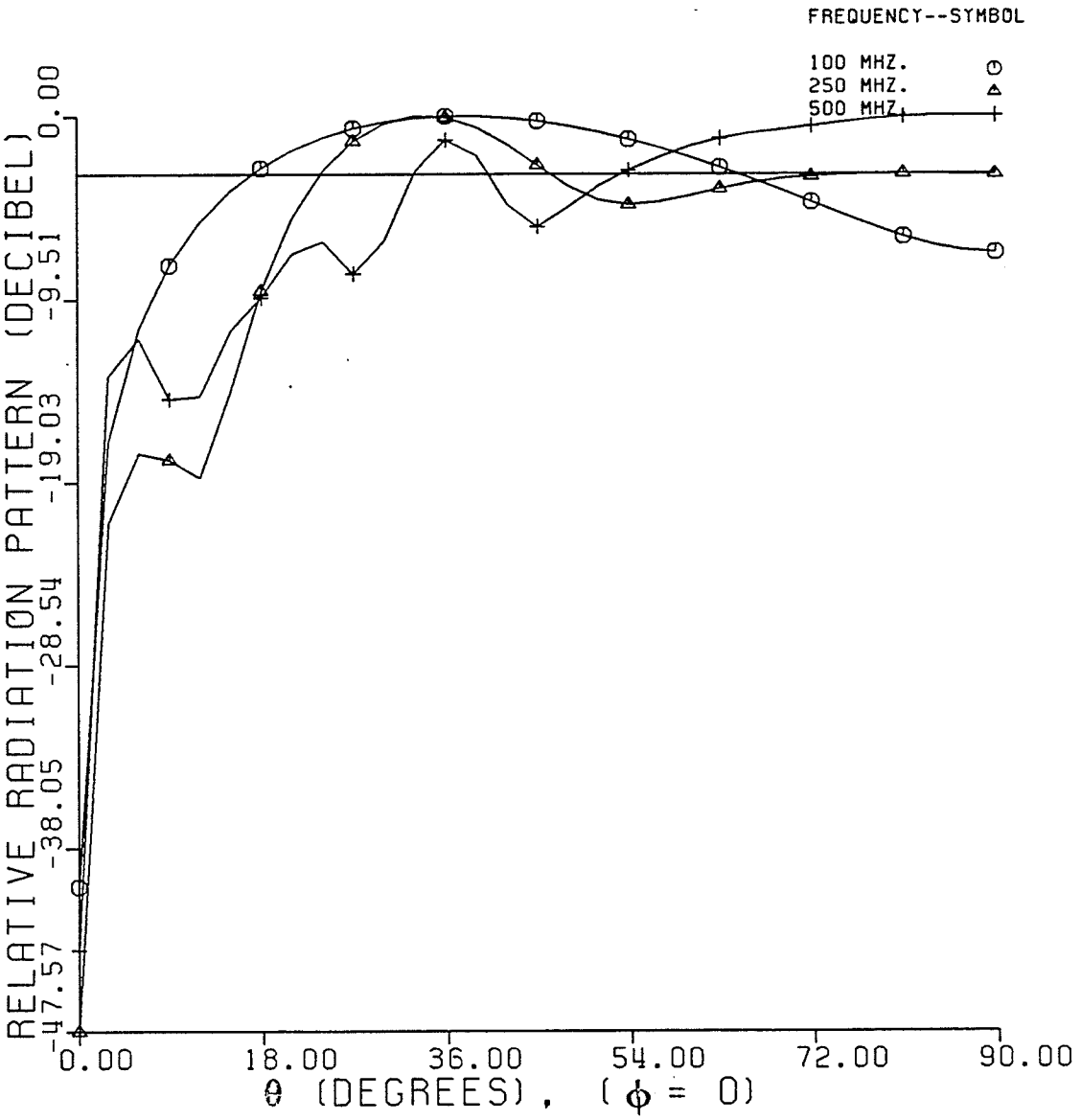

FIG. 5.3: DOMINANT MODE FAR FIELD FOR THE DIRICHLET CONDITION

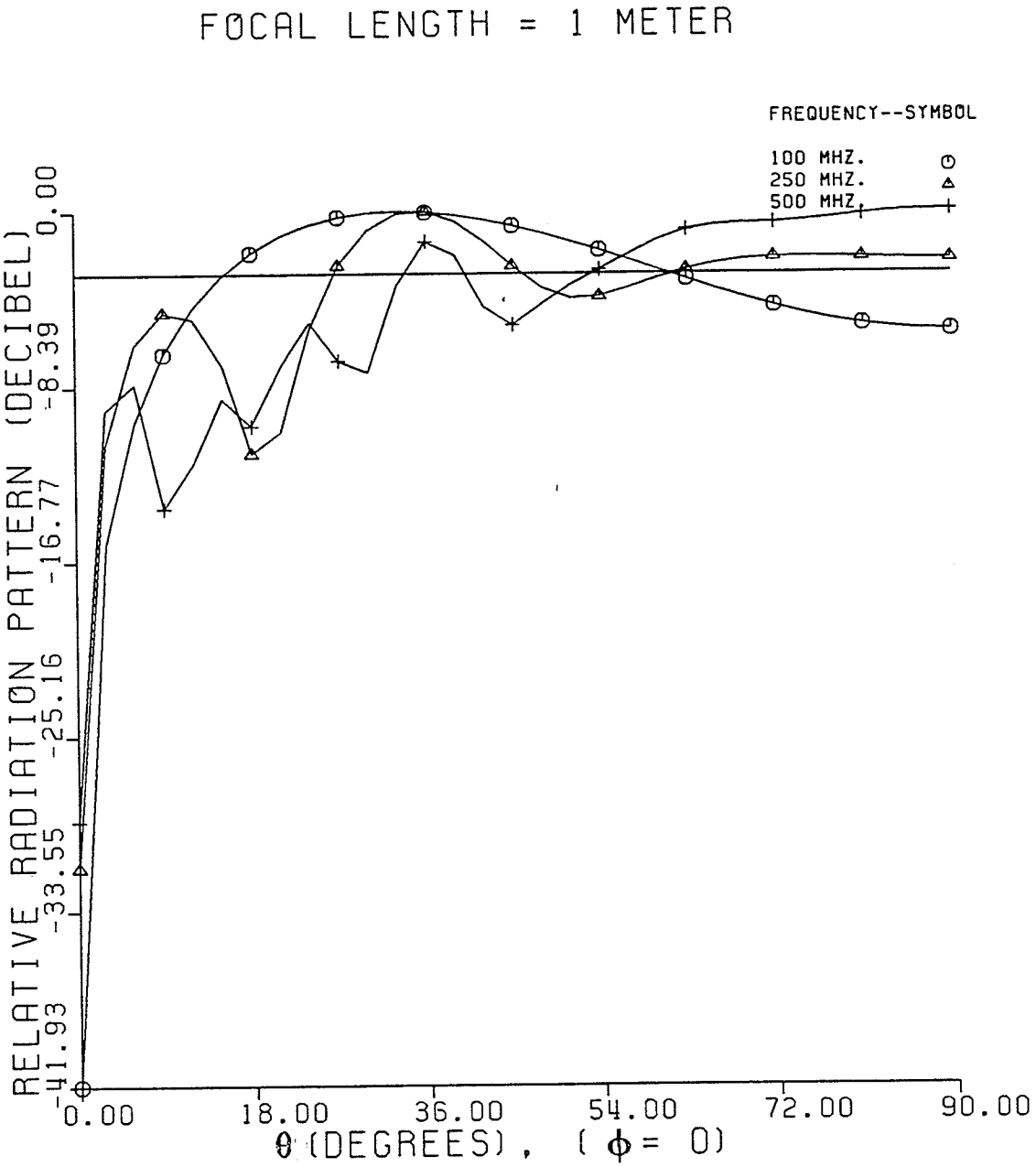

FIG. 5.4: DOMINANT MODE FAR FIELD FOR THE NEUMANN CONDITION

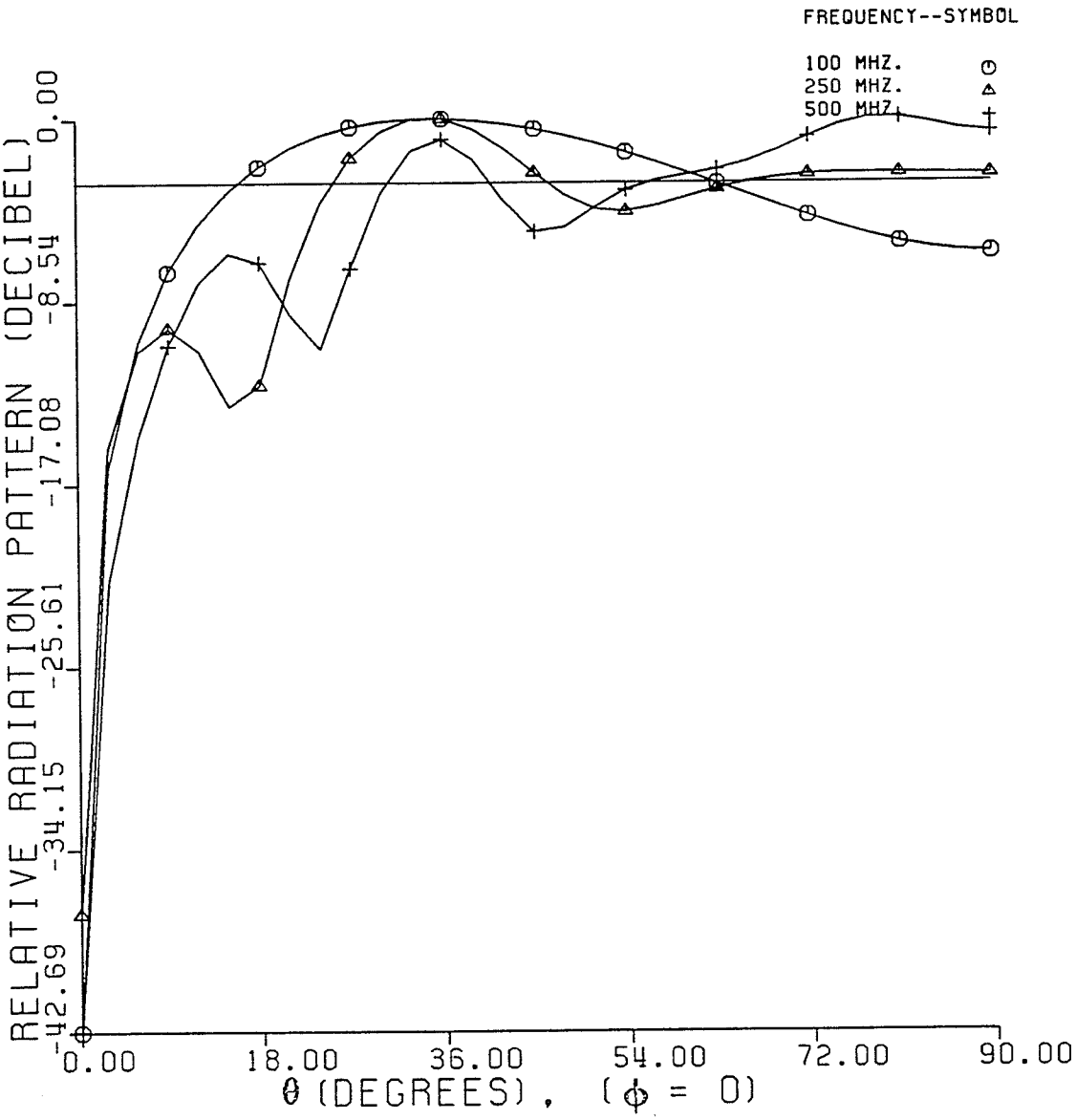

FIG. 5.5: DOMINANT MODE FAR FIELD FOR THE ROBIN CONDITION

CHAPTER 6

CONCLUSIONS

A method has been presented for the evaluation of electromagnetic fields which are independent of ϕ inside a paraboloidal waveguide. The method makes use of the Coulomb wave functions as eigenfunctions for the problem. Although there is little available information on the Coulomb wave functions, their calculation has been achieved with little effort. The procedure is not restricted to the high frequency case as has been shown and thus this is its main advantage. There are no approximations made in the analysis and, except for the assumption that the fields must be independent of ϕ, the analysis is exact. For the case of the finite paraboloid the Kirchhoff approximation was used in the application of Huygen's principle (ie. the incident field for the infinite paraboloid case was used as the Huygen source).

We have found that a finite impedance on the walls of the paraboloid tends to change the far field pattern. specifically the far field pattern seems to be more omnidirectional for the impedance case than for the perfectly conducting case. Whether or not this is a general result will have to wait until further calculations can be made.

Further study is required into the calculation of the irregular Coulomb wave functions for a negative parameter. Once this is done and an efficient computing technique is devised, this method of solving the paraboloidal problem should yield many interesting characteristics. Some of the more important characteristics which are required are the input impedance of the source at the focal point and the difference in radiation pattern due to sources which may be shifted up or down along the axis away from the focal plane.

It is recommended that deep paraboloidal horns are constructed and that experimental radiation pattern results be obtained. Also, since the paraboloid is asymptotically equal to the cone, it is suggested that the possible use of the Coulomb wave functions for the conical horn problem be investigated.

APPENDIX A

THE GENERAL METHOD OF FROBENIUS

In this appendix the general *method of Frobenius* is used to obtain solutions to Eq. (2.37), which is the original differential equation obtained after separation of the partial differential equation. For convenience the differential equation under study is rewritten here with y as the dependent variable, x as the independent variable and λ as the parameter. Thus the equation becomes

$$\frac{d^2y}{dx^2} - \frac{1}{x}\frac{dy}{dx} + \left(K^2x^2 + \lambda\right) = 0\ , \quad x \geq 0\ , \ K \geq 0\ . \tag{A.1}$$

This equation was transformed into a more familiar form in chapter 4 by the transformation

$$z = \frac{1}{2}K\,x^2 \tag{A.2}$$

to obtain the equation

$$\frac{d^2y}{dz^2} + \left[1 + \frac{\lambda}{2Kz^2}\right]y = 0\ . \tag{A.3}$$

From Eq. (A.3) we can immediately see that when $\lambda = 0$ we obtain the complete solution of Eq. (A.1) given by

$$y(z) = A\cos\left(\tfrac{1}{2}Kx^2\right) + B\sin\left(\tfrac{1}{2}Kx^2\right)\ . \tag{A.4}$$

Thus from this point on we will assume that $\lambda \neq 0$.

We now concentrate on solving Eq. (A.1) in the neighborhood of the regular singularity $x = 0$. In applying the method of Frobenius to Eq. (A.1) a solution is

chosen of the form

$$y(x) = x^r \sum_{m=0}^{\infty} c_m x^m \quad , \quad (c_0 \neq 0) \tag{A.5}$$

where the exponent r may be any (real or complex) number and is chosen so that $c_0 \neq 0$ (see Kreyszig [1983], pp. 161).

The assumption that $c_0 \neq 0$ leads us to an important quadratic equation called the *indicial equation*. The roots of the indicial equation corresponding to Eq. (A.1) are 0 and 2. Thus there is a series solution starting with x^2, that is, we assume a solution of the form

$$y_1 = x^2 \left\{ c_0 + c_1 x + c_2 x^2 + \cdots \right\} ,$$

but on substituting this into Eq. (A.1) we soon find that all the odd powers of x vanish. Therefore the series can be written as

$$y_1 = x^2 \left\{ c_0 + c_2 x^2 + c_4 x^4 + \cdots + c_{2r} x^{2r} + \cdots \right\} . \tag{A.6}$$

If we take $c_0 = 1$ after substituting Eq. (A.6) into Eq. (A.1) then we obtain

$$c_2 = -\frac{\lambda}{8} \quad , \quad c_4 = \frac{1}{24} \left(\frac{\lambda^2}{8} - K^2 \right) \tag{A.7}$$

and the three term recurrence relation

$$r(r+2)c_{2r} = -\lambda c_{2r-2} - K^2 c_{2r-4} \quad (r \geq 2) . \tag{A.8}$$

The convergence of the coefficients can be checked from Perron theory of difference equations. Thus we find that

$$\frac{c_{2r}}{c_{2r-2}} = O(r^{-1}) \to 0 \text{ as } r \to \infty .$$

Thus the series given by Eq. (A.6) converges for all finite values of x. This is what we would expect since Eq. (A.1) has no finite singularity other than $x = 0$, so that the power series about $x = 0$ converges for all x with $|x| < \infty$. Hence we have a solution given by Eq. (A.6) with coefficients given by Eq. (A.7) and Eq. (A.8). This solution is comparable to the regular Coulomb wave function obtained in chapter 3 and in fact we see that $y_1 = 0$ at $x = 0$ which was our condition for orthogonality.

The second solution must now be found (ie. the solution corresponding to the root 0). Since the two roots of the indicial equation differ by an integer we expect difficulty in finding the solution which starts with the exponent 0. If we try a solution of the form

$$y_2 = a_0 + a_1 x + a_2 x^2 + \cdots$$

we find that all we get is the solution $y_1(x)$ back again. Thus we look for a logarithmic solution (note that this would be implied from our previouse knowledge) of the form

$$y_2 = y_1 \ln(x) + v(x) \quad . \tag{A.9}$$

On substituting this into Eq. (A.1) we find the equation for $v(x)$ to be

$$v'' - \frac{1}{x} v' + \left(K^2 x^2 + \lambda\right) v = \frac{2y_1}{x^2} - \frac{2y_1}{x} \quad . \tag{A.10}$$

We try solving this by a power series, thus

$$v = b_0 + b_2 x^2 + b_4 x^4 + \cdots \tag{A.11}$$

and we get

$$b_0 = \frac{-2}{\lambda} \quad , \quad b_2 = \textit{arbitrary} \tag{A.12}$$

with the recurrence relation

$$4r(r+1)b_{2r+2} + \lambda b_{2r} + K^2 b_{2r-2} = -2(2r-1)c_{2r} \quad . \tag{A.13}$$

We can take $b_2 = 0$ and get

$$\begin{cases} b_4 = \dfrac{1}{4}\left(\dfrac{K^2}{\lambda} + \dfrac{3\lambda}{8}\right) \\ b_6 = \dfrac{1}{144}\left(K^2 - \dfrac{7\lambda^2}{8}\right) \end{cases} \tag{A.14}$$

with the rest of the coefficients given by Eq. (A.13). Thus we have obtained the logarithmic solution as given by Eq. (A.9) with coefficients given by Eq. (A.13) and (A.14).

It is interesting to see what happens to this second solution as $x \to 0$. Taking the limit as $x \to 0$ of y_2 we find that

$$y_2(0) = \frac{-2}{\lambda} \quad . \tag{A.15}$$

We see from Eq. (3.21) that at $x = 0$ the irregular or logarithmic Coulomb wave function is also a function of λ.

Solving the differential equation by the method of Frobenius has thus yielded the same properties that were found for the solution in terms of the Coulomb wave functions.

APPENDIX B

INVESTIGATION OF THE RECURRENCE RELATION

The recurrence relation given in chapter 3 by Eq. (3.8) is rewritten here as

$$A_{n-2} - \gamma A_{n-1} + n(n-1)A_n = 0 \ . \tag{A.1}$$

where $\gamma = 2\beta$. We can convert this equation into a non-linear first order difference equation by setting $A_n / A_{n-1} = V_n$. This produces the equation

$$1 - \gamma V_{n-1} + n(n-1)V_{n-1}V_n = 0 \ . \tag{A.2}$$

If we assume an asymptotic solution, for large n, of the form

$$V_n \to V = B n^{-\alpha} \ , \tag{A.3}$$

and substitute this into Eq. (A.2) the we arrive at

$$1 - \gamma B n^{-\alpha} + n(n-1)B^2 n^{-2\alpha} = 0 \ .$$

For large n this becomes

$$1 - \gamma B n^{-\alpha} + B^2 n^{2-2\alpha} = 0 \ . \tag{A.4}$$

To eliminate the highest powers of n in Eq. (A.4), we must have $2 - 2\alpha = 0$ which implies that $\alpha = 1$. Thus Eq. (A.4) gives us $1 + B^2 = 0$ which implies that $B = \pm i$. Hence Eq. (A.2) has two asymptotic solutions of order $O(n^{-1})$ so that the general solution of Eq. (A.1) is recessive and the recurrence relation given by Eq. (A.1) is stable.

REFERENCES

Abraham, M. [1900] , *Ann. Phys. Lpz.* , **2** , 32.

Arscott, F.M. and Darai, A. [1981], Curvilinear Coordinate Systems in which the Helmholtz Equation Separates, *IMA J. App. Math.* , **27** , 33-70.

Abramowitz, M. and Stegun, I.A. [1972] , *Handbook of Mathematical Functions* , Dover Pub., Inc., New York.

Balanis, C.A. [1982] , *Antenna Theory Analysis and Design* , Harper & Row, Publishers, New York.

Bowman, J.J., Senior, T.B.A. and Uslenghi, P.L.E. [1969] , *Electromagnetic and Acoustic Scattering of Simple Shapes* , Am. Elsevier Pub. Co., Inc., New York.

Buchholtz, H. [1947], Integral-und Reihendarstellungen fur die vershiedenen Wellentypen der mathematischen Physik in den Koordinaten des Rotationsparaboloids , *Z. Physik* , **124** , 196-218.

Buchholtz, H. [1948], Die axialsymmetrische elektromagnetische Strahlung zwischen konfokalen Drehparabolen bei verschiedenen Anregungsarten , *Ann. Physik* , Ser. 6 , **2** , 185-210.

Donaldson, A.R., French, I.P. and Midgley, D. [1960], Paraboloidal Reflectors with Axial Excitation , *IEE Proceedings* , **107** , Pt. B., 547-552.

Erdelyi, A., Magnus, W., Oberhettinger, F. and Tricomi, F.G. [1953], (Bateman Manuscript Project) *Higher Transcendental Functions, Vol. 1 and 2* , McGraw-Hill Book Co., Inc., New York.

Eisenhart, L.P. [1934], Separable Systems of Staeckel , *Annals of Math.* , **35** , 284.

Fock, V.A. [1965] , *Electromagnetic Diffraction and Propogation Problems* , Pergamon Press, London.

Froberg, C. [1955], Numerical Treatment of Coulomb Wave Functions , *Rev. of Mod. Phys.* , **27** , No. 4, 399-411.

Hadidi, A. [1985], Eigenvalues of Dielectric-Coated Conical Structures, M.Sc. Thesis, Electrical Engineering Dept., University of Manitoba.

Hansen, W.W. [1935], A New Type of Expansion in Radiation Problems , *Phys. Rev.* , **47** , 139-143.

Harrington, R.F. [1961] , *Time-Harmonic Electromagnetic Fields* , McGraw-Hill Book Co., Inc., New York, Chapters 3 & 6.

Horton, C.W. and Karal Jr., F.C. [1950], On the Diffraction of a Plane Sound Wave by a Paraboloid of Revolution , *J. of Acous. Soc. of Am.* , **22** , No. 6, 855-856.

Horton, C.W. and Karal Jr., F.C. [1951], On the Diffraction of a Plane Electromagnetic Wave by a Paraboloid of Revolution , *J. of Appl. Phys.* , **22** , No. 5, 575-581.

Horton, C.W. [1953], On the Diffraction of a Plane Sound Wave by a Paraboloid of Revolution II , *J. of Acous. Soc. of Am.* , **25** , No. 4, 632-637.

International Mathematical and Statistical Library (IMSL) [1982].

Koshlyakov, N.S., Smirnov, M.M. and Glimer, E.B. [1964] , *Differential Equations of Mathematical Physics* , North-Holland Pub. Co., Amsterdam.

Kraus, J.D. and Carver, K.R. [1973] , *Electromagnetics* , McGraw-Hill Book Co., Inc., New York, Chapter 12.

Kreyszig, E. [1983] , *Advanced Engineering Mathematics* , John Wiley & Sons, New York, Chapter 4.

Lamb, H. [1906], On Sommerfeld's Diffraction Problem; And On Reflection by a Parabolic Mirror , *Proc. Lond. Math. Soc.* , **4** , 190.

Love, A.E.H. [1901], The Integration of the Equations of Propogation of Electric Waves , *Phil. Trans. Roy. Soc. London, Ser. A* , **197** , 1-45.

Luk'Yanov, A.V., Teplov, I.V. and Akimova, M.K. [1965] , *Tables of Coulomb Wave Functions (Whittaker Functions)* , The MacMillan Co., New York.

Mackie, A.G. [1965] , *Boundary Value Problems* , Oliver and Boyd, LTD., London.

Mohsen, A. and Hamid, M.A.K. [1970], Wave Propogation in a Circular Waveguide with an Absorbing Wall , *J. Appl. Phys.* , **41** , No. 1, 433-434.

Moon, P. and Spencer, D.E. [1971] , *Field Theory Handbook* , Springer-Verlag, New York.

Morse, P.M. and Feshbach, H. [1953] , *Methods of Theoretical Physics, Vol. I & 2* , McGraw-Hill Book Co., Inc., New York.

National Bureau of Standards [1952] , *Applied Mathematics Series 17, Tables of Coulomb Wave Functions Vol. I* , U.S. Gov. Printing Office, Washington.

Pinney, E. [1946], Laguerre Functions in the Mathematical Foundations of the Electromagnetic Theory of the Paraboloidal Reflector , *J. of Math. and Phys.* , **25** , 49-79.

Pinney, E. [1947], Electromagnetic Fields in a Paraboloidal Reflector , *J. of Math. and Phys.* , **26** , 42-55.

Schensted, C.E. [1955], Electrmagnetic and Acoustic Scattering by a Semi-Infinite Body of Revolution , *J. Appl. Phys.* , **26** , 306-308.

Senior, T.B.A. [1960a], Impedance Boundary Conditions for Imperfectly Conducting Surfaces , *Appl. Sci. Res.* , **B8** , 418-436.

Senior, T.B.A. [1960b], Impedance Boundary Conditions for Statistically Rough Surfaces , *Appl. Sci. Res.* , **B8** , 437-462.

Stratton, J.A. [1941] , *Electromagnetic Theory* , McGraw-Hill Book Co., Inc., New York.

Stutzman, W.L. and Thiele, G.A. [1981] , *Antenna Theory and Design* , John Wiley & Sons, Inc., New York.

Trim, D.W. [1986] , *Partial Differential Equations* , Course Notes, University of Manitoba.

Weston, V.H. [1963], Theory of Absorbers in Scattering , *IEEE Trans.* , **AP-11** , 578-584.

Wilcox, C.H. [1957], Debye Potentials , *J. of Math. and Mech.* , **6** , No. 2, 167-201.